University of Stavanger

Faculty of Science and Technology

MASTER'S THESIS

Study program/ Specialization: Petroleum Technology / Production Technology	Spring semester, 2013 ~~Open~~ / **Restricted access**
Writer: Christer Loddervik	…… (Writer's signature)
Faculty supervisor: Aly Anis Hamouda External supervisor(s): Statoil ASA: Kjetil Skrettingland, Øyvind Myhrer	
Title of thesis: Analyzing zonal well performance measured by production logging from Snorre A.	
Credits (ECTS):	
Key words: Snorre, PI, PLT, SIP, skin, pseudoskin	Pages: 60 + enclosure Stavanger, 14.6/2013 Date/year

Preface

This thesis seeks to investigate zonal well performance on the Snorre A field. The goal is to further understand the value and limitations of the expected performance based on theoretically calculated data versus the actual performance measured by production logging. It is also to give recommendations on how to improve existing theoretical calculations through the use of available data and a better modeling of the skin effects.

The thesis mainly consist of three parts: presenting the Snorre A field, a theory section discussing well performance by the productivity / injectivity indices, and an analysis part including selection of proper data, field calculations based on the theory and comparisons to production logs.

During the time of the thesis professor Aly Anis Hamouda at the University of Stavanger has been of great help discussing theoretical approaches, providing literature, and giving important feedback on the topics of the thesis.

Thanks to Statoil ASA and the Snorre department for providing an interesting thesis topic, and especially to the two Statoil supervisors, Kjetil Skrettingland (leading engineer P-tech) and Øyvind Myhrer (production advisor) for clearing their buzzy schedules to make time for important discussions around the thesis. A special thanks also goes to production specialist Helge Jon Ramstad for being available to answer questions.

Summary

Productivity (PI) is the relative ability to produce oil. The productivity for a well is an indication of the producing quality of the reservoir strata within the drainage radius of the well. For this thesis the well flow performance for each reservoir subzone has been analyzed. Theoretically expected productivity is calculated and compared to actual production logging (PLT) results. Theoretical PI should ideally act as the initial subzone inflow performance parameter. Therefore theoretical data are mainly compared to the initial PLT, but also to later PLT's to evaluate trends through time.

Theoretical PI is given by the formula: $PI = \frac{0.0536\, k_h h}{B\mu\left(ln\frac{r_e}{r_w} - \frac{3}{4} + s_t\right)}$

As seen from the formula above, the PI is dependent on several parameters. Some are easy to determine, while others can be more challenging. Parameters that should be given extra care are the subzone flowing height and the subzone average permeability. This is especially important for highly heterogeneous and anisotropic reservoirs like Snorre. The flowing height is dependent on sufficient permeability.

Looking into log permeability it is the experience that the arithmetic average permeability tends to give an overestimation; while geometric average is seen to give a too low estimate (low numbers included give a large impact being multiplied). Sensitivity analyses were performed selecting different permeabilitymodels and selecting a cutoff to exclude the lowest values in the sands. These low values might be affected by thin shales, or sand/shale transitions. The selected cutoff model was based on an initial geometric average over the chosen sand. The sensitivity analysis showed that selecting the cutoff to 50 % of the initial average, and then calculating a new geometric average yielded a significant improvement in PI estimation accuracy. Cutting away sands with poorer properties (permeability) means reducing the flowing height. This was adjusted for by a net to gross ratio. The main argument for this approach is that the reservoir inflow is largely dominated by the good sands.

Another important variable to determine correctly is the total skin. This thesis presents different types of pseudoskins mainly consisting of perforation (completion) skin, limited flow entry skin, and well deviation skin. Models for calculation each of these pseudoskin components are suggested, along with a formula for calculation of the total skin.

Using the cutoff permeability method and a total skin factor, rather than just the damage skin factor has shown theoretical PI estimations closer to what is seen from the PLT logs.

Theoretical PI estimations based on mobility data has been shown to be of limited value for the producer, while the data is significantly more accurate for the injector. This might be due to wettability and relative permeability effects, since the measured fluid of a mobility drawdown test often is the mud filtrate.

Theoretical values are overestimated for certain subzones. It is expected that the reason for this is smaller reservoir volumes due to faults. The effects of smaller reservoir volume in some of the subzones will be more rapid reservoir pressure fluctuations that again will affect the subzone drawdown.

Contents

1 The Snorre field

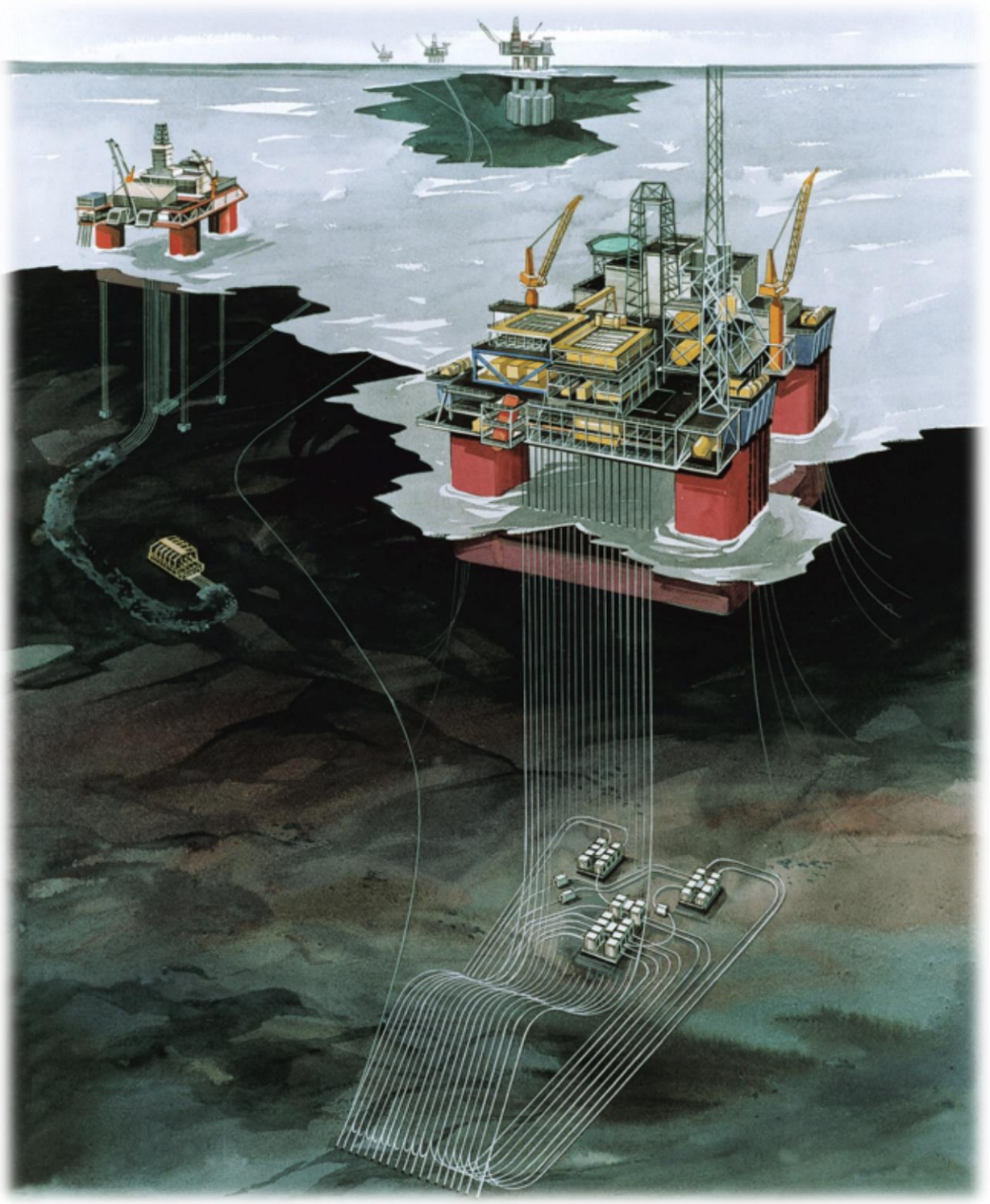

Figure 1: Snorre B in front of Snorre A, Statfjord in the background. Courtesy of Statoil

1.1 Introduction

The Snorre field is located in the Tampen area in the North Sea, west outside the coast of Florø, Norway. It's part of the blocks 34/4 and 34/7 (Figure 2) with Production Licenses 057 and 089, respectively. The field was discovered in 1979 by well NO 34/4-1, and production started with well P-29 in August 1992. Snorre was developed and initially operated by Saga Petroleum. The operatorship was passed on to Hydro at the end of 1999, and then to Statoil in 2002. Daily operations are handled by two floating steel platforms (Figure 3). The first, Snorre A (TLP) in block 34/7, and Snorre B from 2001 in block 34/4 about 7 km north. Both are integrated accommodation, drilling and production platforms. Snorre A also has a subsea template (UPA), and supports the subsea satellite field Vigdis in the same license.

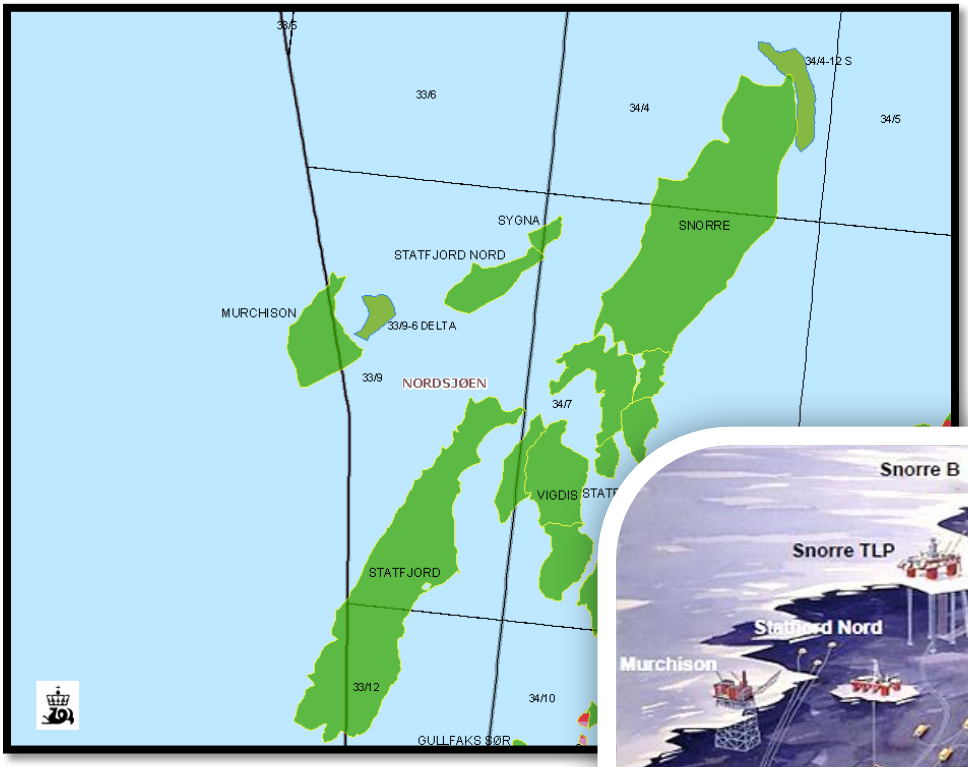

Figure 2 (top): Snorre blocks and surrounding fields. Downloaded from NPD 20.02.2013

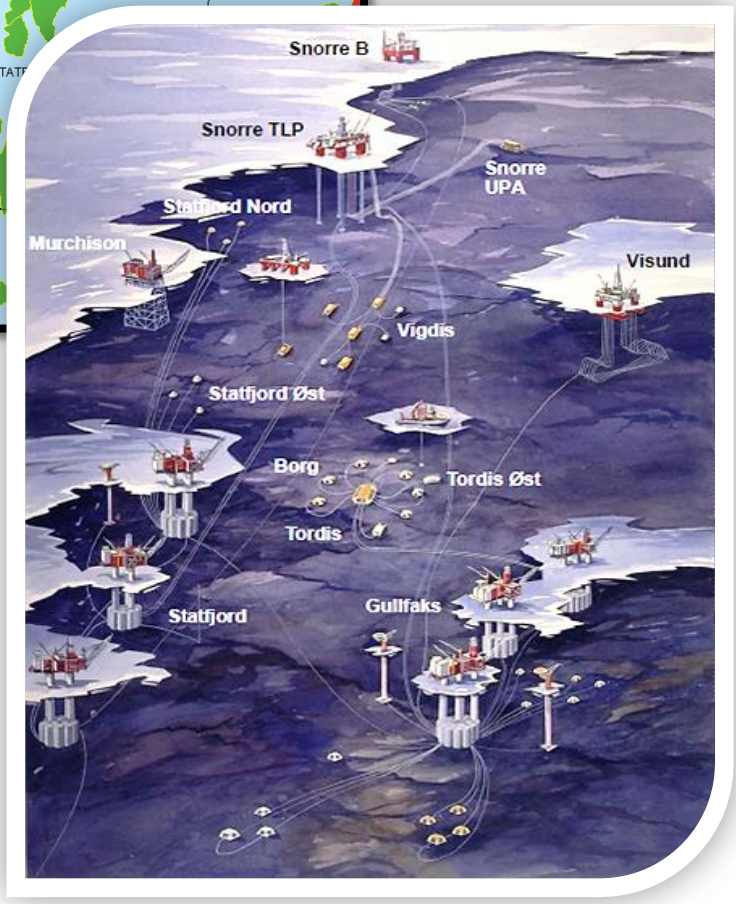

Figure 3 (bottom): Tampen Area installations. Courtesy of Statoil

Snorre is a giant oil producing field, and has over the more than 20 years of production produced 185.8 MSm^3 (200.9 MSm^3 o.e. 2012 numbers, not including Vigdis)[4]. Since the startup the reserves have been more than doubled from about 90 MSm^3 to 251 MSm^3 (266.8 MSm^3 o.e.) [1, 3]. Although Snorre has been producing for a long time, it is the field in Norway with the second most remaining reserves [1, 3]. The platforms Snorre A and B are currently ranked as the fourth highest oil producers in Norway [1]. Development and investments are therefore still ongoing to ensure efficient reservoir drainage and high recovery. This is being done by increased drilling activity (more wells), increased production/process capacity and improved sweep performance. Snorre has been prolonged to continue production to 2040.

Fun Facts, Snorre A [2]:

- *Most producing well: P-23 with 7.57 MSm^3*
- *Production record 07.des.06 with almost 30.000 Sm^3/d*
- *Highest well production rate: P-18 25.mar.94 with 5900 Sm^3/d*
- *46 well slots + 10 subsea*

1.2 Reservoir

The Snorre field is situated in the north-eastern part of the East Shetland Basin, within the northern crest of the Tampen Spur. The Tampen Spur is a major late Jurassic to early Cretaceous structural high, consisting of a series of large west to north-westward rotated fault blocks located between the Viking Graben to the east and south-east, and the Møre Basin to the north and north-west. The Snorre Fault Block, holds both the Snorre field, and also the Tordis and Vigdis fields. In contrast to the other giant fields on the Tampen Spur, the Snorre field has reservoir rock restricted to the Triassic Lunde Fm. and Triassic-to-Early-Jurassic Statfjord Gp. [4] (plus BRENT Gp. and Draupne Fm. in the south for Tordis/Vigdis). The reservoir has a complex sand/shale structure of heterogeneous stratified fluvial sandstone with many alluvial channels and internal flow barriers. The depositional environment is marine and fluvial, and believed to be a combination of alluvial plain, shallow lake/bay settings, meandering rivers and deltas (Figure 4). The complexity from channels and faults makes various sand connectivity and pressure barriers together with variable N/G, porosity and permeability.

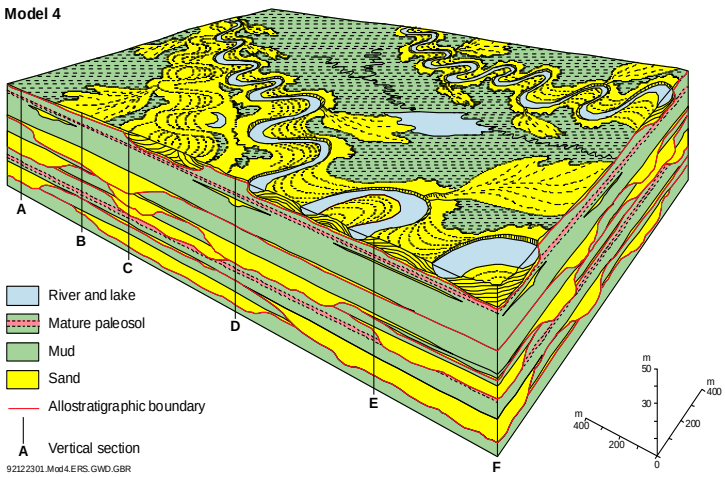

Reservoir sands are filled with light undersaturated oil, and have a weak natural aquifer.

Figure 4: Snorre depositional model. Courtesy of Statoil.

1.2.1 Reservoir blocks

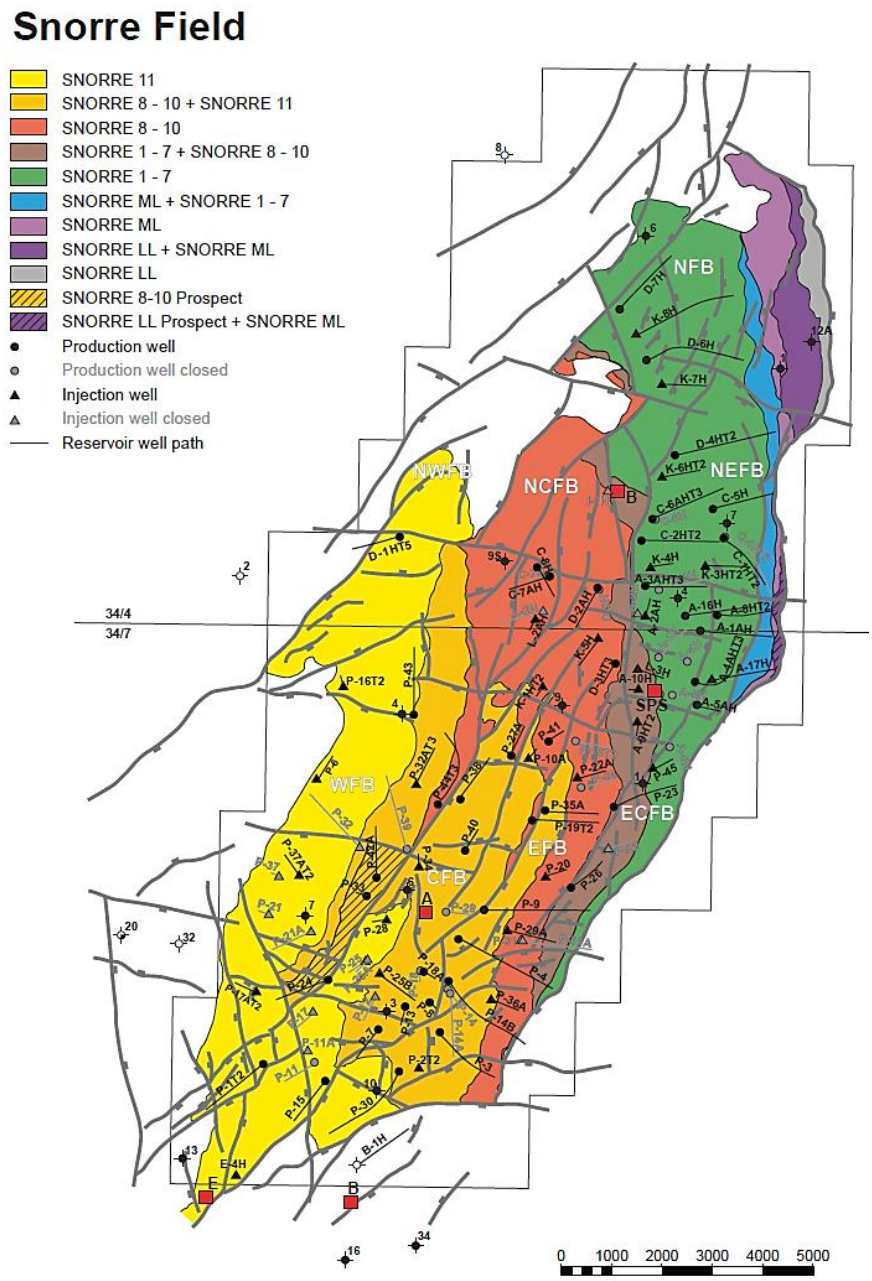

Figure 5: Snorre field map with fault blocks. Courtesy of Statoil.

Major faults like the Murchison Fault, Outer Snorre Fault (OSF), Inner Snorre Fault (ISF), and Central Snorre Fault (CSF) divide the reservoir into blocks. From west the blocks are the West Fault Block (WFB - yellow), North-West Fault Block (NWFB - yellow), Central Fault Block (CFB - orange), North Central Fault Block (NCFB - red), East Fault Block (EFB), East Central Fault Block (ECFB - brown), North Fault Block (NFB - green), and the North-East Fault Block (NEFB) as shown on Figure 5. All these faults exhibit dip slip to the east, and are subdivided into branches that partly overstep each other. These many faulted segments contribute to reduce communications between producers and injectors, especially on zones with low N/G [5].

1.2.2 Reservoir zones

Reservoir blocks are divided vertically into numbered zones, determined by different reservoir sands. This is observed from a hierarchy of cyclicity interpreted from cores. It is the short term cycles that defines the main reservoir zones that range from a thickness of 40 – 140 m. Pressure and production data are also incorporated in the reservoir zonation. The most important pressure barriers are normally reservoir zone boundaries. From the bottom reservoir these zones are the Middle Lunde member (ML) and the Upper Lunde member and Statfjord Fm. strata divided into Snorre 1-11 (often denoted SN1-11). The zones are again each divided into 4 subzones. Zones are represented with various occurrences in the respective blocks, as shown in Figure 6. It varies between the blocks which zones are hydrocarbon bearing, and how they contribute with oil and water production.

Key Numbers [5]***:***

- *Reservoir depth: ~2500 m TVD*
- *Max. gross thickness: 1000 m*
- *N/G: ~45 %*
- *Reservoir temperature: ~90 °C*
- *Initial res. pres.: 383 bar*
- *Porosity: 14 – 32 %*
- *Permeability: 100 – 4000 mD*

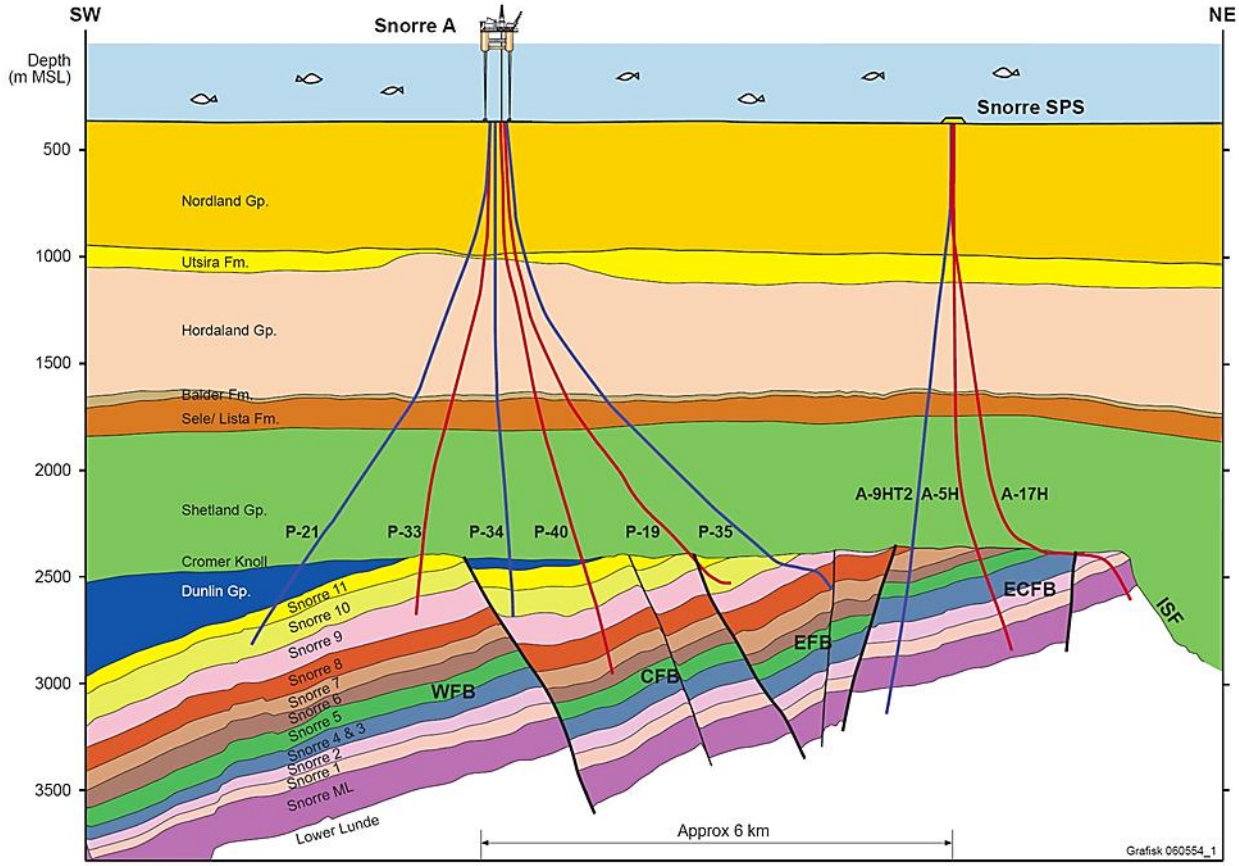

Figure 6: Snorre reservoir zones. Courtesy of Statoil.

1.2.3 Drainage strategy

The main Snorre reservoir drainage strategy is displacement of oil, and pressure maintenance by water and gas injection. Currently the goal for voidage replacement ratio is between 1.0 and 1.1, hence maintaining or increasing reservoir pressure to secure well productivity, avoid sand production and drilling and completion problems. The field was originally developed with water injection as drainage strategy but early in the field life modified to water alternating gas (WAG) injection through advanced well completions. These completions include inflow control valves (ICV) and extensive downhole instrumentation in order to handle the variable nature of the individual sand deposits, as shown on figure 7. WAG is mainly performed in downdip locations. The current installations typically comprise four ICV's per well and is remote operated either hydraulically or electric/hydraulically. Later years there are pressure and temperature gauges for each ICV both on the tubing and annulus side which give comprehensive data acquisition for well and reservoir diagnosis and for production optimization. In addition to the data acquisition aspects the applications are used for selective water or gas injection on the injection side and for choking high GOR and WC on the producer side. One of the goals is maximizing gas injection on Snorre.

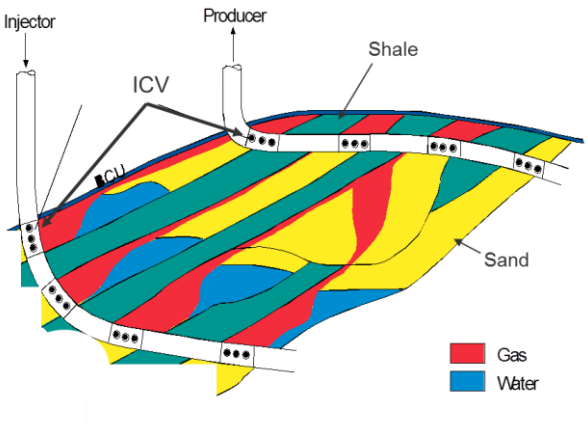

Figure 7: WAG on ICV wells. Courtesy of Statoil.

Another important technology for reservoir management on Snorre has been the use of time lapse (4D) seismic. Eight conventional surface seismic surveys have been acquired since 1983, with 3-8 years between the seismic vintages. A Permanent Reservoir Monitoring (PRM) system with optical cables installed on the seabed has just been approved for the Snorre field to improve the seismic time resolution down to every few months. The goals are [4]:

- Mapping secondary gas caps
- Map changes in oil/water contact (OWC) level
- Localize undrained compartments and reservoir zones
- Map communication across faults
- Map pressure and overburden changes

The above information will be used both in well planning and well interventions, and by production and injection management.

1.3 Challenges & Data acquisition

In a highly stratified fluvial system, like Snorre, one of the main challenges is to provide adequate recovery from all zones. First priority data to be acquired are thus data on zonal contribution and zonal pressure. Data on the efficiency of the flooding process is of increasing importance. Data acquisition with respect to quantifying residual oil saturation, the solubility of injected gas and the relative mobility of the reservoir fluids are given high priority. Data that has the potential to reduce the uncertainty of the initial volume of oil in place or improve the understanding of the reservoir are also given priority.

The first data gathering on Snorre started with the seismic interpretation in 1983, which has been further developed into 4D seismic through later seismic runs. A lot of data like gamma ray/resistivity, density/neutron, sonic, dipmeter data, coring, formation pressure and cement logs are gathered during drilling and completion of new wells. From the more advanced Modular formation Dynamics Tester (MDT) tools permeability and mobility information are estimated through a probe being injected into the formation and withdrawing a fluid sample while measuring local drawdown and buildup data [15]. The drawdown pressure depends on mobility.

After completion of wells pressure and temperature data are closely monitored and stored. All of the wells have pressure and temperature sensors both at the wellheads, and downhole. Wells with ICV have more advanced gauge instrumentation. Attempts to replace gauges by Prosper calculations have been shown to be too inaccurate. On Snorre downhole pressure gauges are recommended installed in all new wells.

Well production at the Snorre field is measured using test separators. Wells are normally tested every month. The production test results are analyzed and validated with well hydraulics software. Based on the validated production test a well performance curve is made. The well performance curves are used in the daily production allocation process to distribute production from the separators to the respective contributing wells.

Analysis of produced fluids helps in determining the state of the drainage process. The ion composition in water shows the split between formation water and injected water. The asphaltene content in the oil may show the degree of dissolved gas by the oil. After water breakthrough samples for ion analysis and H_2S measurements are performed regularly. Due to patterns of injection water breakthrough and reservoir conditions, the potential for scale formation in most wells in the Snorre field is low. In some formations there are instances of scale formation which have required either preventive or remedial treatment. The scale management strategy at Snorre has been a reactive treatment strategy, where no reservoir treatments for scale inhibition were performed until well production data or ion data indicated signs of potential scale development. If there were indications of scale development, scale inhibitor squeeze treatment usually in combination with scale dissolver was performed. Lately a more proactive approach is implemented. This means that wells that are considered to be at risk will be treated before there is a loss in productivity.

An extensive tracer injection and monitoring program is used in the Snorre reservoir. The data has provided useful information on breakthrough times and pathways (including cross fault communication) for both water and gas injection, and has assisted in a better understanding of the WAG process.

As pressure is declining sand production is becoming a larger problem on Snorre. Most of the producing wells are producing sand, and are limited by sand production. Sand production are monitored both due to erosion of the equipment, and to ensure that the wells are producing above the sand lifting rate to ensure that the sand are being transported out of the well and avoid settling and accumulation in the wellbore. On both Snorre A and B this is done by acoustic sand detectors (particle monitors). These are calibrated annually by injecting a known amount of sand. Acceptable sand free tests are performed regularly to maximize production from sand producing wells.

Snorre has run about 120 production logs (PLT) over the years to quantify the zonal injection and production per well. PLT logs are internally recommended ran initially, at first water breakthrough, and thereafter as required by operational and reservoir management needs. Since PLTs is the main part of this thesis it will be discussed in detail in a separate section.

1.3.1 Other limitations

Historically increasing WC has limited oil production on Snorre A through water handling capacity. In 2009 modifications were made to more than double this capacity. Snorre B is not affected by water handling. WAG steering of the injectors is done to maintain the WC on the producers at a reasonable level. When this method is insufficient, or when the produced water handling capacity has been reached, the strategy is to choke back high WC wells and reduce water inflow by ICV operation or performing an intervention.

Snorre B has in periods been limited by gas volumes due to increasing GOR. In this period gas was exported to Snorre A for injection. Snorre A currently also uses gas from Vigdis for injection, and is not limited by gas handling capacity. Generally the field GOR is increasing, but is expected to be reduced with proper WAG cycles. Maintaining WC and reducing GOR is done by optimal timing of the WAG cycles to keep water/gas coning at a minimal level.

H_2S is assumed to occur in the near wellbore region of injection wells during seawater injection. The H_2S is then transported in the reservoir fluids to the producing wells. H_2S is currently not a constraint for production, but significant increase is expected in the future. In order to meet the specification for the gas export from Snorre A to Statfjord A, chemical H_2S scavenger is added to the separators. Nitrate treatment of the injected water has shown to be an efficient way of decreasing the H_2S level.

2 Theory – flow performance

2.1 Productivity / injectivity index (PI / II)

Productivity is the relative ability to produce oil. The productivity for a well is an indication of the producing quality of the reservoir strata within the drainage radius of the well. It is a measure of the producing formation, and does not take into account the resistance of the flowing string. Some of the mathematical steps in the following section may be simplified and incomplete, and are intended only to show the assumptions and simplifications along the way of deriving the formula for productivity index.

For a closed reservoir block it is assumed that reservoir parameters and production/injection is constant. For the time interval that is relevant for the calculations these are fairly good assumptions. This will lead to pseudo steady state conditions after some time, which is defined by pressure change proportional to the elapsed time both in the reservoir and in the well.

$$\frac{\partial p}{\partial t} = constant \neq 0$$

For practical calculations it is assumed that the reservoir subzones has constant thickness (h). When the area (A) and porosity (ϕ) is constant the total porevolume (V) is defined by:

$$V = \phi hA$$

The produced volume is given by:

$$\Delta V = \frac{qBt}{24}$$

Where B is the formation volume factor, and the constant 24 accounts for rates (q) given in Sm^3/d and elapsed time (t) given in hours. Total system compressibility, c_t, can be defined from the latter two equations:

$$c_t = \frac{1}{V}\frac{\Delta V}{\Delta p} = \frac{1}{\phi hA}\frac{qBt}{24\,\Delta p(t)}, \qquad \Delta p(t) = p_i - \bar{p}(t)$$

Flowequation without gravitational forces:

$$\frac{\partial}{\partial x}\left(\frac{k_x \rho}{\mu}\frac{\partial p}{\partial x}\right) + \frac{\partial}{\partial y}\left(\frac{k_y \rho}{\mu}\frac{\partial p}{\partial y}\right) + \frac{\partial}{\partial z}\left(\frac{k_z \rho}{\mu}\frac{\partial p}{\partial z}\right) = \frac{\partial}{\partial t}(\phi\rho)$$

Converted to radial flow towards the well:

$$\frac{1}{r}\frac{\partial}{\partial r}\left(r\frac{k_r \rho}{\mu}\frac{\partial p}{\partial r}\right) + \frac{\partial}{\partial z}\left(\frac{k_z \rho}{\mu}\frac{\partial p}{\partial z}\right) = \frac{\partial}{\partial t}(\phi\rho)$$

Assuming permeability is constant throughout each direction (k_r = const. ≠ k_z). This is a fair assumption for the singlephase flow of undersaturated oil in the Snorre reservoir. If the reservoir boundaries can be set to r = constant and z = constant the geometric (horizontal) average permeability can be found as:

$$k_h = (k_{r1}k_{r2} \dots k_{rn})^{1/n}$$

With k_h now representing horizontal permeability, and changing k_z to the more used k_v for vertical permeability. Using this, the previous equation simplifies to:

$$\frac{1}{r}\frac{\partial}{\partial r}\left(r\frac{\rho}{\mu}\frac{\partial p}{\partial r}\right) + \frac{k_v}{k_h}\frac{\partial}{\partial z}\left(\frac{\rho}{\mu}\frac{\partial p}{\partial z}\right) = \frac{1}{k_h}\frac{\partial}{\partial t}(\phi\rho)$$

The right hand side of the latter equation can be derived to:

$$\frac{\partial}{\partial t}(\phi\rho) = \rho\frac{\partial\phi}{\partial t} + \phi\frac{\partial\rho}{\partial t} = \phi\rho\left(\frac{1}{\phi}\frac{\partial\phi}{\partial p} + \frac{1}{\rho}\frac{\partial\rho}{\partial p}\right)\frac{\partial p}{\partial t} = \phi\rho c_t\frac{\partial p}{\partial t}$$

Assuming constant compressibility and viscosity, the result from the derivation above leads to:

$$\frac{1}{r}\frac{\partial}{\partial r}\left(r\rho\frac{\partial p}{\partial r}\right) + \frac{k_v}{k_h}\frac{\partial}{\partial z}\left(\rho\frac{\partial p}{\partial z}\right) = \frac{\phi\mu\rho c_t}{k_h}\frac{\partial p}{\partial t}$$

Using the isotherm compressibility (c), the density can be eliminated by assuming compressibility and pressure changes are small:

$$c = \frac{1}{\rho}\frac{\partial\rho}{\partial p}$$

This together with the assumption that the flow is pure radial ($\partial p/\partial z = 0$) and that r has the boundary r = r_e, and wellbore radius is r_w, simplifies the equation to:

$$\frac{1}{r}\frac{\partial}{\partial r}\left(r\frac{\partial p}{\partial r}\right) = \frac{\phi\mu c_t}{k_h}\frac{\partial p}{\partial t}$$

Inserting for c_t as expressed previously and uses that ($\partial p/\partial t$) = constant:

$$\frac{1}{r}\frac{\partial}{\partial r}\left(r\frac{\partial p}{\partial r}\right) = \frac{qB\mu}{\pi(r_e^2 - r_w^2)k_h h}$$

Rearranging and integrate r ∂r:

$$r\frac{\partial p}{\partial r} = \frac{qB\mu}{\pi(r_e^2 - r_w^2)k_h h}\frac{r_e^2}{2} - \frac{qB\mu}{\pi(r_e^2 - r_w^2)k_h h}\frac{r^2}{2}$$

$r_w << r_e$ which leads to:

$$\frac{\partial p}{\partial r} = \frac{qB\mu}{2\pi k_h h}\left(\frac{1}{r} - \frac{r}{r_e^2}\right)$$

Integrating this equation from r_w to r gives [6]:

$$p(r,t) - p_{wf}(t) = \frac{qB\mu}{2\pi k_h h}\left(ln\frac{r}{r_w} - \frac{r^2}{2r_e^2}\right)$$

Again assuming $r_w << r_e$ and averaging the pressure over the reservoir give an expression for drawdown:

$$\bar{p}(t) - p_{wf}(t) = \frac{qB\mu}{2\pi k_h h}\left(ln\frac{r_e}{r_w} - \frac{3}{4}\right)$$

Also accounting for the skineffect (s_t) the above expression becomes:

$$\bar{p}(t) - p_{wf}(t) = \frac{qB\mu}{2\pi k_h h}\left(ln\frac{r_e}{r_w} - \frac{3}{4} + s_t\right)$$

The productivity index is defined as the producing rate divided by the drawdown:

$$PI = \frac{q}{\bar{p} - p_{wf}}$$

Inserting the drawdown expression including skin, and including a factor for SI-units:

$$PI = \frac{0.5429\ k_h h}{B\mu\left(ln\frac{r_e}{r_w} - \frac{3}{4} + s_t\right)}$$

In Statoil SI-units are common for engineering applications, but permeability is usually given in mD and pressure in Bar. This can be accounted for with a new factor:

$$PI = \frac{0.0536\ k_h h}{B\mu\left(ln\frac{r_e}{r_w} - \frac{3}{4} + s_t\right)}$$

All the assumptions are done as simplifications to match the limited input data that often are available and to get an expression without coefficients that are dependent on pressure. The flowequations discussed in this section are fundamental for analyzing welltests from pressuretransient data. Even though it contains a lot of assumptions and simplifications the well pressure will (after a transition period) follow a solution for a sufficient amount of time so that the connection between pressure, time and key parameters can be analyzed [6].

2.1.1 Formation thickness

As seen from the formula above, the formation thickness is an important parameter to determine correctly in order to calculate an accurate PI. Although the reservoir is divided into zones and subzones, one subzone usually consists of both shales and sands. Layers of sand with sufficient porosity and permeability for production are called netsand. Some subzones may have thin netsands that has not been perforated. If these are sufficiently separated by shale from perforated netsands, crossflow is not likely and the sands will not be counted as contributors. Since the reservoir in Snorre has a not negligible dip, the thickness used is the true stratigraphic thickness (TST) of the contributing netsands. This is the

thickness measured at a 90 degree angle to the stratigraphic surface, and equals the true vertical depth (TVD) for a no-dip reservoir.

2.1.2 Pseudoskin

Skin is a term used to describe pressure drop in the near-well formation. It is usually given as a dimensionless factor, where zero skin equals the initial formation. Positive skin indicates flow restrictions that result in a pressure drop larger than initial, and negative skin indicate stimulation that has resulted in a lower pressure drop than the original formation. It is not uncommon that the reservoir has some mechanical formation damage after the drilling due to particles from the mud. This is what is normally referred to as skin, here called damage skin (s_d). The value of damage skin is normally evaluated from transient analysis of a pressure buildup test and can be seen as an early time-pressure deviation from a plotted straight line in a Horner plot.

However there also exist some types of pseudoskin that may play an important part. The pseudoskin factor is a time-independent quantity for times exceeding the start of pseudoradial flow. The most important of these are skin from perforations, limited flow entry skin and skin due to well deviation. When calculating the productivity index it is important to account for all these types of skin with a total skin factor (s_t).

2.1.2.1 Perforation skin

The selection of proper perforating hardware (perforator and gun type) is essential for optimizing productivity in perforated completions. Pressure drop caused by restrictions on how the fluid enters the well through the perforations is considered as a pseudoskin called perforation skin, s_p. Perforation skin accounts for the pressure drop caused by the flow through the perforations (dependent on perforation length and diameter), flow through a crushed formation around the perforations with reduced permeability, and changes in the flow pattern caused by the density and phasing between the perforations. The shot density is important for changes in the flow in the vertical direction, while the phasing (angle) is important for changes in horizontal flow. Multidirectional perforations offer significant advantages over unidirectional perforations [16].

These pseudoskin effects become increasingly important as the perforation diameter and length decreases, crushed zone thickness increases (and crushed zone permeability decreases), as the shot density gets lower and the phasing gets larger. See figure 8 below:

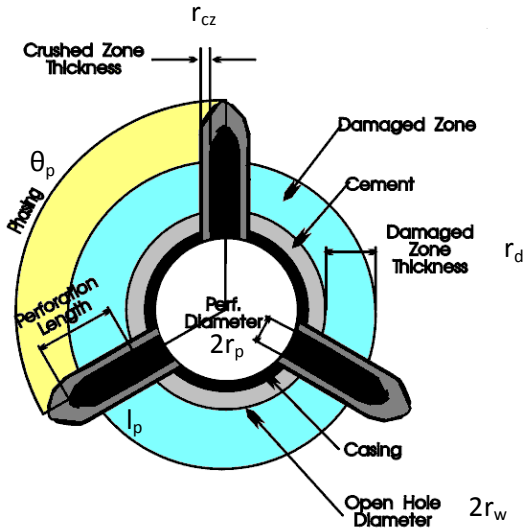

Figure 8: Perforation skin properties. From IPM's Prosper Manual.

IPM's Prosper recommends using the Karakas and Tariq correlation model [16] for perforation skin. This model takes into account all the different skin components discussed above:

Horizontal skin component:

$$s_h(\theta_p) = ln\left[\frac{r_w}{\alpha_\theta(r_w + l_p)}\right]$$

Where θ_p is the horizontal phasing angle between the perforations, r_w is the wellbore radius, l_p is the perforation length, and α_θ is a table value.

Vertical skin component:

$$s_v = 10^{a_1\, log\left[\frac{r_p}{2h_s}\left(1+\sqrt{k_v/k_h}\right)\right]+a_2} \cdot \left[\frac{h_s}{l_p}\sqrt{k_h/k_v}\right]^{\left[b_1\frac{r_p}{2h_s}\left(1+\sqrt{k_v/k_h}\right)+b_2\right]-1} \cdot \left[\frac{r_p}{2h_s}\left(1+\sqrt{k_v/k_h}\right)\right]^{b_1\frac{r_p}{2h_s}\left(1+\sqrt{k_v/k_h}\right)+b_2}$$

Where a_1, a_2, b_1 and b_2 are table values, r_p is the perforation radius, and h_s is the vertical spacing between the perforations.

Wellbore skin:

$$s_{wb}(\theta_p) = c_1 \cdot e^{c_2\left[\frac{r_w}{r_w+l_p}\right]}$$

c_1 and c_2 are table values. All table values are given in the appendix.
Crushed zone skin:

$$s_{cz} = \frac{h_s}{l_p}\left(\frac{k}{k_{cz}} - 1\right) ln\left(\frac{r_{cz}}{r_p}\right)$$

k_{cz} and r_{cz} are the permeability and radius of the crushed zone, respectively.

Total perforation skin:

$$\boldsymbol{s_p = s_h + s_v + s_{wb} + s_{cz}}$$

Damage skin can also be included in the model:

$$s_{p+d} = \left(\frac{k}{k_d} - 1\right) ln\left(\frac{r_d}{r_w}\right) + \left(\frac{k}{k_d}\right) s_p$$

k_d and r_d are the permeability and radius of the damaged zone, respectively.

The permeability related to the vertical flow, and especially damaged zone and crushed zone permeabilities are not always known. Karakas and Tariq propose a set of guidelines to estimate these values:

- Vertical permeability: 10 % of reservoir permeability
- Damaged zone permeability: 25 % of reservoir permeability
- Crushed zone permeability: 50% of reservoir permeability

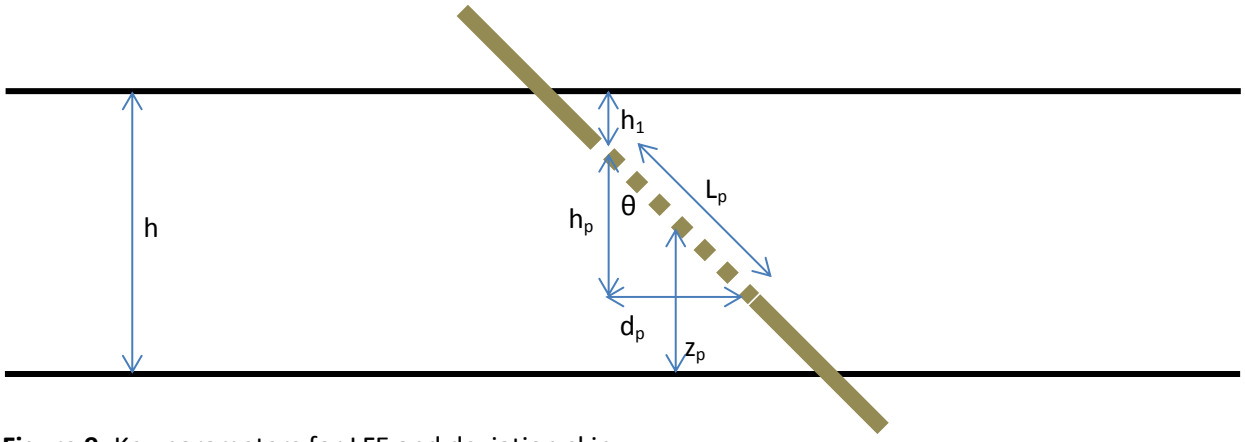

Figure 9: Key parameters for LFE and deviation skin.

2.1.2.2 Limited Flow Entry (LFE)

For some wells certain zones might not be perforated throughout the entire netsand thickness, as illustrated in figure 9 above. This might be due to plugged perforations, or the completion might be designed this way to delay water (or gas) coning. In these cases the flow cannot be pure radial, and flowlines are forced to converge vertically toward the open well. Deviation in the flow pattern results in a longer distance of travel, and a higher resistance of flow than that of uniform radial flow. Vertical permeability is in most cases less than horizontal permeability due to deposition. This is usually accounted for through a k_v/k_h ratio, where k_v is the vertical permeability, and k_h is the horizontal permeability. Boundary effects from the impermeable top and bottom layer are also accounted for.

Because of this, pressure responses show an additional pressure drop that reduces the well productivity compared to a well fully penetrating the netsand. At late times, the additional pressure loss can be accounted for by a lumped quantity of pseudoskin often called LFE-skin or partial penetration skin (s_{LFE}). In wells with limited flow entry the precise quantification of this additional pressure drop is of paramount importance to completely identifying formation damage.

Various expressions exist to account for this type of skin. In 1968, Odeh presented a correlation for LFE-skin based on steady-state flow in a finite reservoir. He later (1977) used a finite cosine transform to derive an analytical solution for pseudosteady-state flow of a well with limited entry, and in 1980 he developed an equation for calculating skin factor due to restricted entry [7]. Streltsova-Adams (1979) solved the LFE problems with Laplace and Henkel transformations and derived a skin expression with infinite sine and cosine series [8]. As figure 8 illustrates, these expressions account for thickness of the producing interval, location of the open interval (middle of perforation to bottom netsand), length of the open interval and the wellbore radius. S_{LFE} is most sensitive to the formation thickness and the length of the perforated interval. Large formation thickness with a small perforation interval will cause a large pressure drop. On the other hand, when the perforation height (h_p) approaches the total thickness of the producing layer (h) there will be no LFE-skin. The effects of LFE-skin also become more apparent as the difference in k_h and k_v increases.

In 2008 a comprehensive investigation was performed by Gui et al [9] comparing available models listed in the literature used for estimation of pseudoskin due to limited flow entry. The study show that the trend is that LFE-skin calculated with the Streltsova-Adams formula yields the largest effect, while calculation with the Odeh formula gives the smallest LFE-skin. Further discussion of LFE-skin will therefore focus on these two models.

The two models both start from the differential equation for the flow in an anisotropic compressible oil formation mentioned earlier, where vertical flow needs to be allowed:

$$\frac{1}{r}\frac{\partial}{\partial r}\left(r\frac{\partial p}{\partial r}\right)+\frac{k_v}{k_h}\frac{\partial^2 p}{\partial z^2}=\frac{\phi\mu c_t}{k_h}\frac{\partial p}{\partial t}$$

Odeh found that the LFE-skin factor as a function of sand thickness, location of the open interval, and the wellbore radius can be estimated by the equation:

$$s_{LFE}=1.35\left(\left(\frac{h}{h_p}-1\right)^{0.825}\left\{ln\left(h\sqrt{\frac{k_h}{k_v}}+7\right)-\left[0.49+0.1\,ln\left(h\sqrt{\frac{k_h}{k_v}}\right)\right]\cdot ln\left[r_w e^{0.2126\left(\frac{h-z_p}{h}+2.753\right)}\right]-1.95\right\}\right)$$

The correlation is constructed for oilfield units. Odeh does not indicate the range of validity for the equation.

Streltsova-Adams first made the differential flow equation dimensionless and solved it with Laplace and Henkel transforms with boundary conditions saying initial reservoir pressure is uniform and that the layers over and under the producing sand is impermeable. Uniform flux is also assumed in the perforated interval. The result is an expression for well pressure which is integrated to find an average

value. It is an expression with a two-part sum where the first part is the normal transform expression for a fully perforated well. Hence the second part must represent the LFE-skin:

$$s_{LFE} = \frac{2h^2}{\pi^2 h_p^2} \sum_{n=1}^{\infty} \frac{1}{n^2} \left\{ \sin\left[\frac{n\pi}{h}(h_p + h_1)\right] - \sin\left[n\pi \frac{h_1}{h}\right] \right\}^2 K_0 \left(\frac{n\pi r_w}{h\sqrt{\frac{k_h}{k_v}}} \right)$$

K_0 represents the modified Bessel function of the second type and zero order. This slowly converging infinite equation is solved by computer programs.

The mathematical derivations are too complex to be given focus here, but are available in reference [6] and [8].

Lee et al presented a new method for computing pseudoskin factor for a partially-penetrating well in 2001 [10], with the aim of providing a simple method for estimating LFE-skin factor regardless of the complexity of the reservoir, location of the open intervals or the number of layers. It also requires a minimum of assumptions on the reservoir geometry, and little computational effort. This method also builds upon the diffusivity equation for radial flow, and the derivation of the drawdown expression showed earlier (with the same assumptions), but at a dimensionless state.

To make the previous drawdown expression dimensionless we introduce dimensionless pressure defined as:

$$p_D = \frac{2\pi k_h h}{q\mu}(p_{wf} - p)$$

Using this, the expression for dimensionless drawdown for a fully perforated well becomes:

$$(\bar{p}_D - p_{wfD})_c = -\left(ln\frac{r_e}{r_w} - \frac{3}{4} \right)$$

The pseudoskin factor is determined from the difference between the dimensionless drawdown between a fully (denoted c) and a partially (denoted p) perforated well:

$$s_p = (\bar{p}_D - p_{wfD})_c - (\bar{p}_D - p_{wfD})_p$$

The dimensionless drawdown for the partially perforated well has to be found from production data.

2.1.2.3 Well deviation skin

Many wells do not penetrate the producing layer perpendicularly. Instead there is a deviation angle between the wellbore axis and the stratigraphic surface. Because of a higher contact surface between the well and the formation, this situation creates an increase in well productivity compared with vertical wells [11]. This effect can be handled as a pseudoskin factor (s_θ) with a negative value. In 1975 Cinco et al

developed a correlation that is a function of the well deviation angle and is proportional to the logarithm of the formation thickness [12]:

$$s_\theta = -\left(\frac{\theta}{41}\right)^{2.06} - \left(\frac{\theta}{56}\right)^{1.865} log\frac{h_p}{100r_w}$$

This is valid for a fully perforated isotropic reservoir where $0° \leq \theta \leq 75$, $h_p/r_w > 40$ and the dimensionless time, $t_D > 100$.

Dimensionless time is defined as: $t_D = \frac{0.0036\, k_h t}{\phi \mu c_t r_w^2}$ in SI units.

For anisotropic reservoirs that have directionally dependent permeability, the deviation skin equation has to be modified by changing the well projection and angle [6]:

$$h'_p = h_p \left(\frac{k_h}{k_v}\right)^{1/3}$$

$$d'_p = d_p \left(\frac{k_v}{k_h}\right)^{1/6}$$

$$\theta' = \tan^{-1}\left(\sqrt{\frac{k_v}{k_h}}\tan\theta\right)$$

Inserting this in the deviation skin equation gives:

$$s_\theta = -\left(\frac{\tan^{-1}\left(\sqrt{\frac{k_v}{k_h}}\tan\theta\right)}{41}\right)^{2.06} - \left(\frac{\tan^{-1}\left(\sqrt{\frac{k_v}{k_h}}\tan\theta\right)}{56}\right)^{1.865} log\left[\frac{h_p}{100r_w}\left(\frac{k_h}{k_v}\right)^{1/3}\right] + s_\alpha$$

Where s_α is the skin caused by the changed well shape, defined as:

$$s_\alpha = \cos\left[\tan^{-1}\left(\sqrt{\frac{k_v}{k_h}}\tan\theta\right)\right] ln\frac{2\sqrt{\cos^2\theta + \frac{k_v}{k_h}\sin^2\theta}}{1+\sqrt{\cos^2\theta + \frac{k_v}{k_h}\sin^2\theta}}$$

Petex's Prosper recommends this Cinco correlation model for well deviation up to 65°. For highly deviated wells the Wong-Clifford skin model should be selected. The Wong Clifford model is not relevant for this thesis, so it will not be further discussed. More information can be found in reference [13] and [14].

The angle, θ, is shown in figure 9, and is the normal definition of a deviation angle. It is worth noting that for a dip reservoir all parameters are given with respect to the stratigraphic surface. This means that horizontal permeability in reality is radial permeability parallel to the same surface, which is logical since the layers are deposited horizontal and altered later. Because of this, and that the reason for deviation skin is due to larger reservoir contact, the well deviation angle also has to be given relative to the stratigraphic surface.

2.1.2 Total skin

To determine the well condition and correctly estimate the productivity index, it is necessary to correct the skin not only for well damage, but also to include the effects of the completion, limited flow entry and well deviation. For this a total skin factor, s_t, which includes all flow restrictions near the well is useful. The total skin factor may have a positive or a negative value. Thus a deviated well with limited flow entry may appear stimulated or damaged compared to a fully perforated vertical well. When evaluating skin damage from the apparent skin from a pressure buildup test it is important to be aware of LFE and the effects of deviation, as it can completely change the picture on whether or not stimulation should be applied. The formula for total skin can be approximated by [6]:

$$s_t = s_p + s_{LFE} + \frac{h}{h_p} s_d + s_\theta \left(\frac{L_p}{h}\right)^{2.7}$$

Which is valid for $L_p \leq h$. For $L_p > h$, the effect of limited flow entry becomes less important and when the well is close to fully perforated LFE-skin can be neglected without significant error.

The equations are also valid for injectors. However if water is being injected into an oilzone the above equation must be modified to account for the difference in mobility between the water and oil phases and the relative permeability effects [9]. This is done by multiplying the above equation with a mobility ratio:

$$M_{ow} = \frac{\frac{k k_{rw}(1 - S_{or})}{\mu_w}}{\frac{k k_{ro}(S_w)}{\mu_o}}$$

where k_{rw} and k_{ro} are relative permeability for water and oil, respectively. S_w is the water saturation, and S_{or} is the residual oil saturation.

2.2 Inflow Performance Relation (IPR)

The inflow performance relation for a well is the relationship between the flowrate of the well and the flowing bottomhole pressure. It is normally used to assess well performance, but can also be used for other applications. The data required to make an IPR-curve are obtained by measuring the production rates under various drawdown. For a single phase (incompressible) undersaturated oilwell it will plot as a straight line, as illustrated in figure 10:

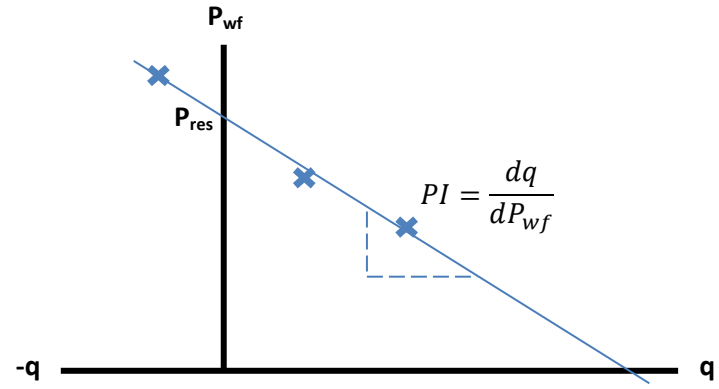

Figure 10: IPR illustration and key information.

The gradient of the line is the productivity index, and the point where the line crosses the ordinate represents the true average reservoir pressure. Whenever we have a production log, these two relations are extremely important. From a production log with more than one rate (including shut-in), the straight line can be made. Real data might deviate a bit from the straight line, so it is preferred to have at least three rates and use linear regression to reduce uncertainty. If there is a shut-in measurement with no crossflow between the zones, this would give the reservoir pressure directly. From a production log it is possible to get P_{res} and PI information on a subzone level. An interpretation like this is called a **selective inflow performance (SIP)** analysis. It is used as the most accurate measure available of the zonal performance and production distribution. Knowledge about this is important for optimal reservoir drainage through accurate production / injection allocation. It is also important for production optimization, especially as the watercut increases, and can be used for well interventions like reperforation, plugging or setting of a straddle (blocking off a zone, while producing through the plug). SIP should be used with caution on injectors, due to possible fracturing and rate/pressure-dependent injectivities.

2.3 Production logging (PLT)

Although theoretically calculated values may give an indication of the zonal performance and distribution of produced volumes, the only way to get this information for sure is through production logging. It is also used as key information to evaluate completion efficiency, clean-up and qualify properties like permeability and skin (transient testing). Production logging becomes even more important when there is more than one flowing phase, and calculations and simulations become increasingly complicated and uncertain.

Production logging is performed by running a special wireline tool consisting of several measure devices, as shown in figure 11. Modern tools can also measure multiphase flow. It is usually run several times upwards and downwards across the producing intervals at different but constant cable speeds. Normal cable speeds are 10, 20, 30 and 40 m/min. If the well exceeds approximately 60° deviation it is often the case that the logging tool cannot descend to the required depth by gravity alone. This is due to friction and the reduced vertical weight component (weight * cos θ). In Statoil it is most common to use a tractor to provide the additional required force, but coiled tubing, pipe conveyance or pumping the tool down are also options.

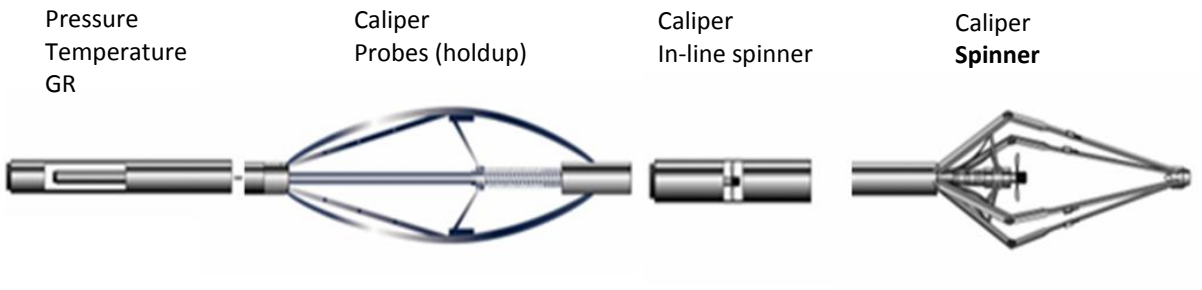

Figure 11: Typical PLT string. Courtesy of Statoil.

The toolstring is equipped with sensors to take measurements that allow calculation of zonal flow contributors by phase. Typical sensors in a PLT are:

Gamma Ray (GR): Although the length of the wire running the tool is measured, the GR tool is essential for depth correlation in the well. It is also used to detect radioactive scale (Barium or Strontium Sulphate)

Pressure and temperature sensors: Used for PVT and key information for formation pressure and drawdown calculations. Temperature sensors are also good indicators of flow.

Gradio manometer: Accurate tool to measure fluid density and water holdup. Can only be used if the well deviation is less than 60°.

Holdup (y) is defined as the fraction of a fluid present in an interval of the pipe. It is not the same as the cut from the flowrate, since lighter phases tend to move faster than the heavier phases (slip). E.g. for oil/water flowing the oil holdup is defined as: $y_o = A_o/(A_o + A_w)$ where A denotes the cross-sectional area covered by oil and water. Flowregimes are again determined from the holdup information.

Gas Holdup Optical Sensor Tool (GHOST): Optical tool that distinguish between liquid and gas, and gives gas holdup. It uses a photodiode that measures light reflection through a sapphire needle from the tip/fluid interface. The reflection is high in gas, and low in liquid. Its use is limited (due to probe blinding) when there is wax or asphaltenes present in the well.

Reservoir Saturation Tool (RST): Used to find holdup of oil, water and gas. The tool consists of an electric neutron generator that measures carbon/oxygen ratio in the well fluid.

Caliper: Important for tool centralization and for correct inner diameter (ID) measurements. The tool usually consists of a multifinger caliper, with at least four (x,y) calipers.

Spinner: Spinner is the most important part of the PLT string. It is a small propeller that will rotate because of the relative movement between the PLT and the fluid, and is hence directly proportional to the fluid velocity. For a spinner there is usually a threshold ($v_{threshold}$), meaning a certain necessary (relative) fluid velocity before the spinner will start to rotate. For liquids this is around 2 m/min. A PLT string usually consists of two spinners: one in-line spinner (backup) and the main one at the end of the toolstring. The spinners have to be calibrated in no-flow conditions before every run to obtain the correlation (slope) between the spinner rotation velocity and the wireline speed (v_{cable}). This is used to find the *apparent fluid mixture velocity (v_{app})*:

$$v_{app} = \left(\frac{spinner\ RPS}{slope\ from\ spinner\ cal.}\right) + v_{threshold} - v_{cable}$$

The apparent fluid velocity has to be adjusted by a velocity profile correction factor (VPCF) to account for the difference in flow profiles between laminar and turbulent flow. The value is usually approximated as 0.9. The *average fluid mixture velocity (v_{mix})* can then be found as:

$$v_{mix} = v_{app} \cdot VPCF$$

Flow correlations provide slippage velocities which, in combination with v_{mix}, allow phase velocities (v_i) to be calculated for phase *i*. Since the area (A) of the tubing (ID) is known, the phase rates (q_i) can be calculated by:

$$q_i\ [m^3/min] = v_i[m/min] \cdot A[m^2] \cdot y_i$$

A stable wellstream is important before running the PLT. Running passes are performed at shut-in to detect crossflow, and at one or more flowing rates. Interpretation of the logging data are performed in simulation software. Statoil currently use Emeraude by Kappa Engineering.

3 Analysis

3.1 Objects

The closed reservoir segment being analyzed is the Central Fault Block (CFB) of Snorre A. This reservoir segment exerts a 10 degree dip compared to a horizontal reservoir. The drainage strategy in the southern part, where the chosen wells are located, is down-dip water injection. The plan is that injectors are placed close to or below the free water level, and the producers as far updip as possible.

Two wells have been chosen for analysis: one producer (P-8), and the supporting injector (P-12). The wells are the first wells drilled in this reservoir segment, with the producer being active about one year before the startup of the injector. Initial wells have been chosen to eliminate the number of uncertainties from effects of surrounding wells. Another reason for choosing these wells is the good amount of data available. Both of the wells have been extensively logged, and their reservoir sections have been cored where directional permeability has been measured at several points. Detailed production tests (buildup) and logs (PLT) are available before and after the startup of the injector. This is believed to be a good basis for the analysis.

The well production/injection performance is being analyzed on a subzone level. Productivity is therefore looked at as a sum of the contribution from all of the perforation intervals from each subzone.

3.2 Wells

3.2.1 Producer, P-8:

The producer, named P-8, runs through the reservoir with a 8.5" hole and a 45° deviation angle. It is fully perforated through the payzones of subzones SN 10.3, SN 10.2, SN 10.1, SN 9.4 and SN 9.3 (increasing depth). Payzones is defined as producible sands with sufficient hydrocarbon (oil) volumes.

From an early transient pressure buildup test the drainage radius (r_e) and damage skin (s_d) has been determined.

A schematic overview of P-8 is given in figure 12, key data used in the analysis is given in table 1, and a Computer Processed Interpretation (CPI) log is given in figure 13:

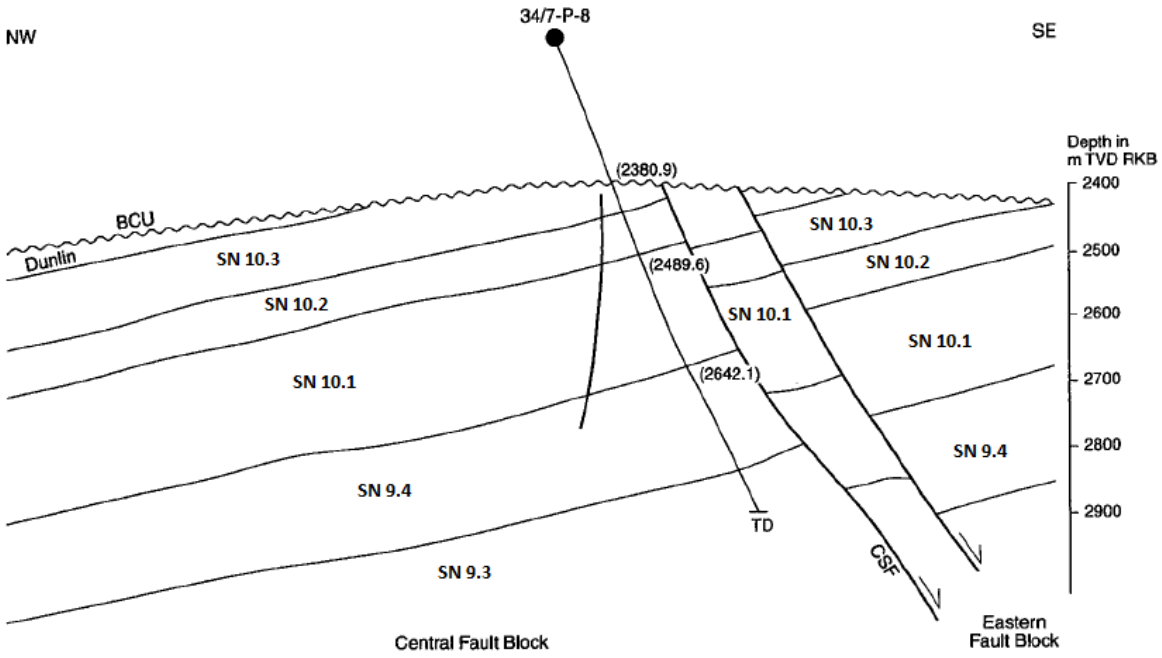

Figure 12: Wellpath through reservoir sections, showing subzones and dip of layers. Courtesy of Statoil.

Well radius, r_w	0.10795 m (4.25 in)
Drainage radius, r_e	950 m
Oil viscosity, μ_o	0.79 cP
Oil formation volume factor, B_o	1.265 m^3/Sm^3
Anisotropic permeability factor, k_v/k_h	0.205
Damage skin, s_d	1.2
Well deviation angle (reservoir), θ	45°
Perforation shot density, h_s	12 /ft
Perforation shot phasing, θ_p	30°

Table 1: Key data used in analysis for well P-8 and reservoir.

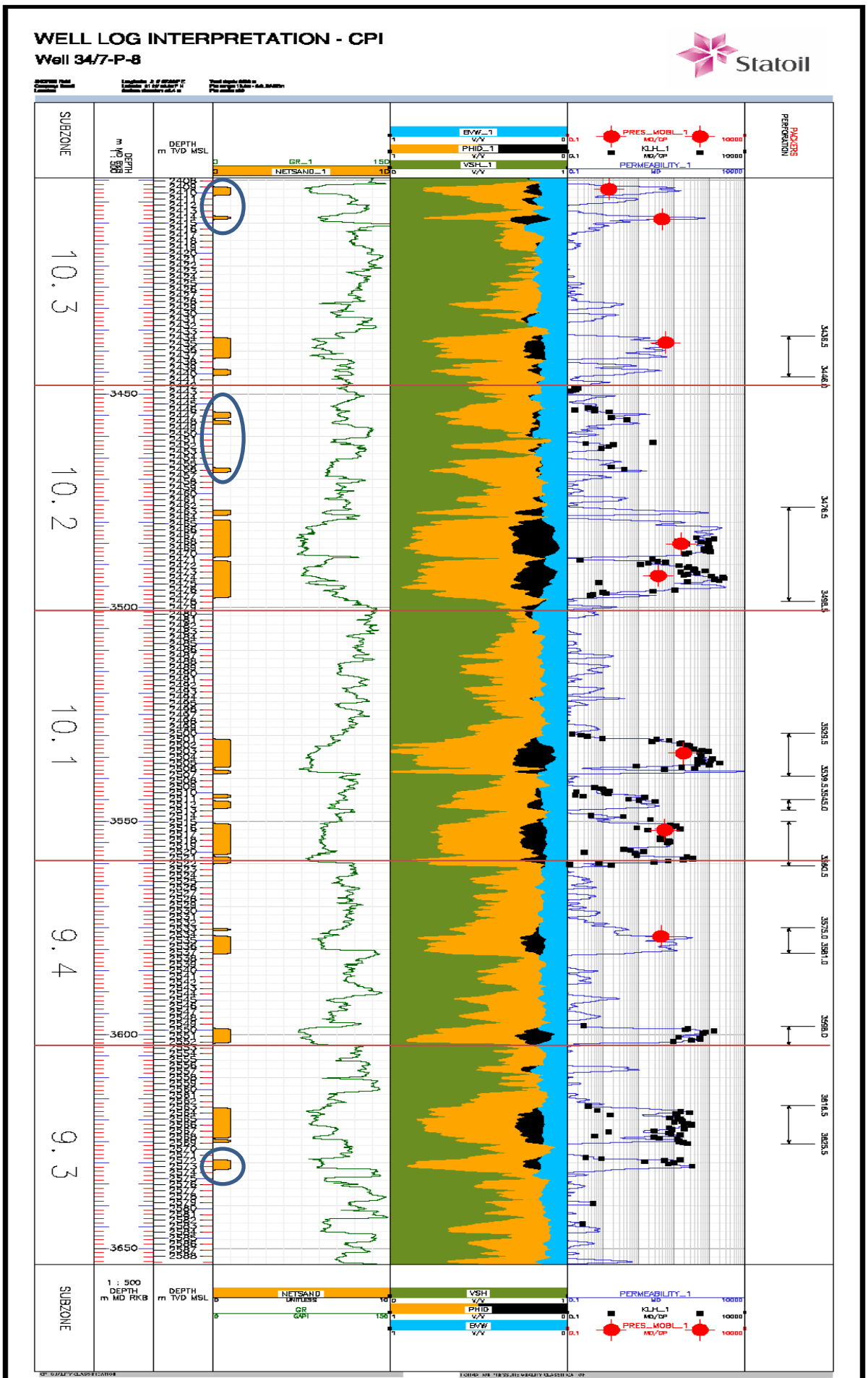

Figure 13: P-8 CPI-log. Courtesy of Statoil

3.2.2 Injector, P-12:

The injector, named P-12, is located west of the producer. Like the producer the reservoir was drilled with a 8.5" bit and a 45° deviation angle. P-12 was fully perforated through the netsands of subzones SN 10.2, SN 10.1, SN 9.4 and SN 9.3. This means subzone SN 10.3 is not supported by the injector, mainly because it is located above the OWC.

From an early transient pressure buildup test the drainage radius (r_e) and total skin (s_t) has been determined.

A schematic overview of P-12 is given in figure 14, key data used in the analysis is given in table 2, and a CPI-log is given in figure 15:

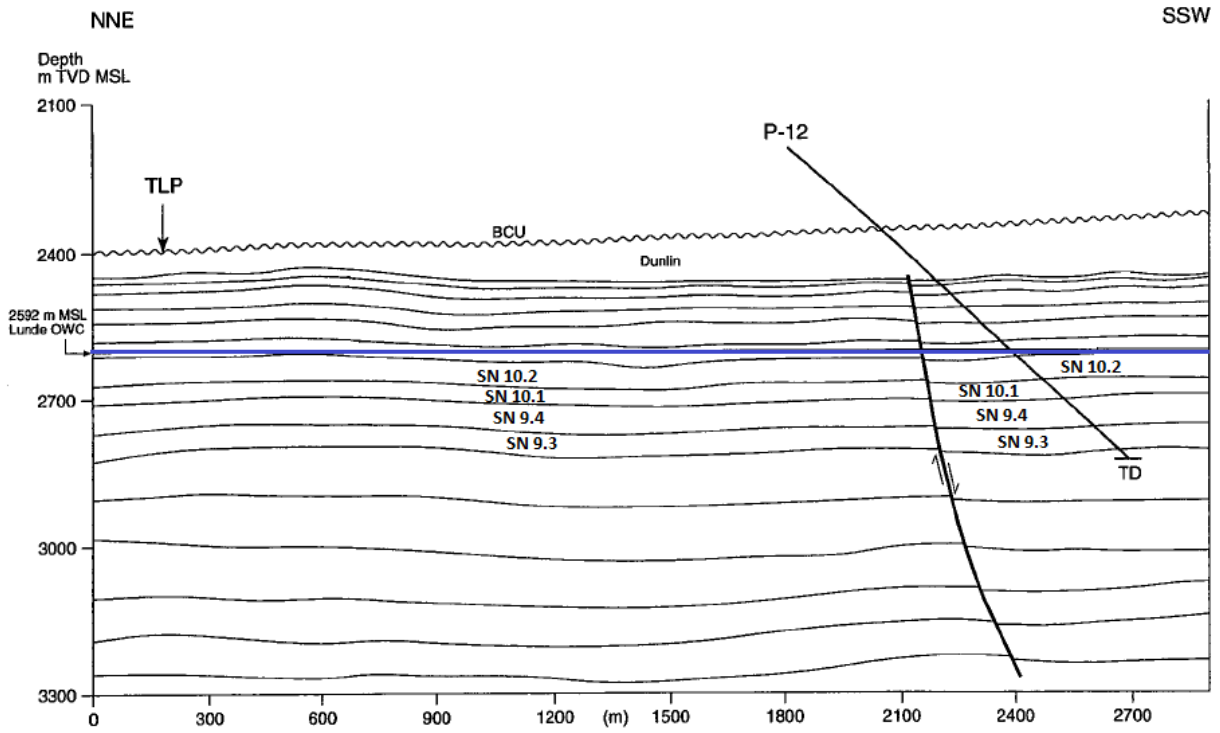

Figure 14: Wellpath through reservoir sections, showing subzones and OWC. Courtesy of Statoil.

Well radius, r_w	0.10795 m (4.25 in)
Drainage radius, r_e	950 m
Water viscosity, μ_w	0.95 cP
Water formation volume factor, B_w	1.02 m^3/Sm^3
Anisotropic permeability factor, k_v/k_h	0.205
Total skin, s_t	-4.05
Well deviation angle (reservoir), θ	45°
Perforation shot density, h_s	12 /ft
Perforation shot phasing, θ_p	30°

Table 2: Key data used in analysis for well P-12 and reservoir.

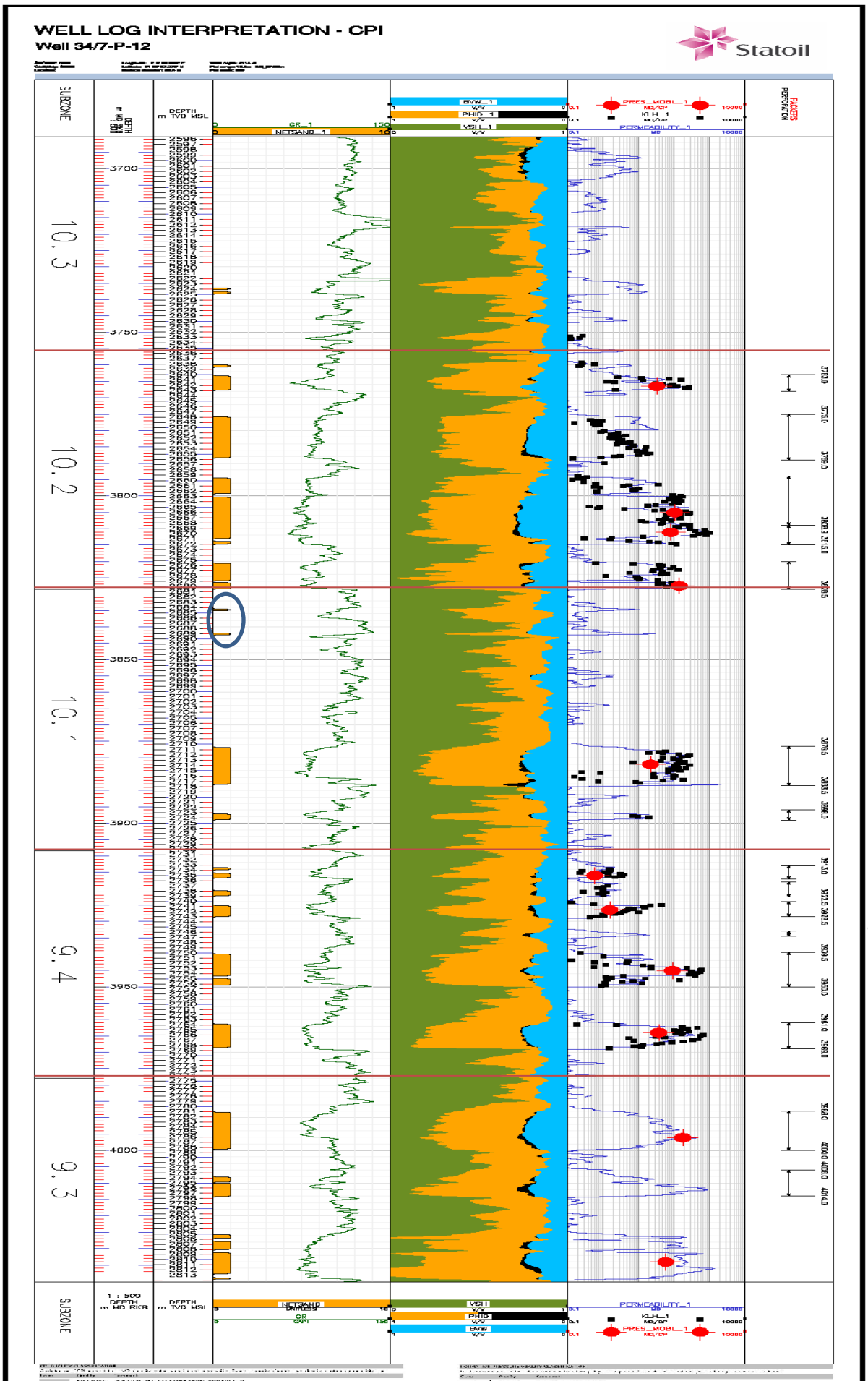

Figure 15: P-12 CPI-log. Courtesy of Statoil

3.3 Permeability

Horizontal permeability as geometric averages together with k_v/k_h-ratio for each subzone was originally provided by the petrophysicists. Arithmetic averaged permeability on the Snorre field is thought to be too optimistic. However calculations in this thesis showed that the provided (horizontal) permeability was too conservative.

Looking into the CPI-plot, the relevant subzones are shown at the far left column of the plot. Log permeability is shown as the continuous curve in the rightmost column, before the perforation intervals in the right margin. The log permeability is tuned against the measured core permeability, shown as black dots in the same plot. Comparing the log permeability against the perforation intervals, for example for the perforation interval of P-8's subzone 10.2, it is clearly seen that impurities in the sand from shale and boundaries in the perforation interval would affect the average permeability. These effects would be apparent, but they would not limit the good sands. The geometric average gives much weight to such low values. It is also known that permeability measurements are more commonly underestimated than overestimated. Because of this it is proposed to set a cutoff value to exclude values that are under a certain limit from the geometric average within the subzone. This also corresponds to corrections done to the subzone height. Another argument for manipulating the permeability this way is that for the sake of reservoir flow, experience show that the highly permeable sands are dominant for zonal performance.

Both provided permeability, and permeability calculated by the new method is listed in table 3 below:

Subzone	P-8 [mD]	P-12 [mD]
SN 10.3	31	-
SN 10.2	141	23
SN 10.1	93	44
SN 9.4	107	16
SN 9.3	79	73

Subzone	P-8 [mD]	P-12 [mD]
SN 10.3	19	-
SN 10.2	489	70
SN 10.1	197	79
SN 9.4	195	36
SN 9.3	120	73

Table 3: Permeability used in the analysis. The top section shows the provided values, while the bottom section is the new interpretation with 50 % cutoff of initial geometric average (for each subzone).

3.4 Mobility

Local mobility estimates are found in the same plot as permeability, and are shown as red dots. These measurements are performed at chosen locations where the MDT-tool has taken local drawdown pressure samples. The mobility estimate applies to a relatively small area around the probe, and normally the measured fluid sample will be the mud filtrate. Using more than one measuring probe eliminates most of the near-probe effects, but still this measurement has some limitations. The mobility estimate is shown to be better for (water) injectors than for (oil) producers. Mobility data are given in in table 4:

Subzone	P-8 [mD/cP]	P-12 [mD/cP]
SN 10.3	60.6	-
SN 10.2	161.8	82.2
SN 10.1	124.6	55
SN 9.4	44.1	45.2
SN 9.3	-	60.0

Table 4: Mobility estimates used in the analysis.

Some of the zones have more than one drawdown pressure sample. For these zones the data was evaluated based on the continuous log permeability. Samples taken outside the perforation interval are ignored. Samples taken at peak or dip permeability are roughly adjusted. For zones with several measurements at different perforation intervals, the values have been evaluated, and weighted according to the perforation interval length.

3.5 Netsand and subzone height

Next to the subzones in the CPI-plot, depth scales in both MD and TVD MSL can be found. After these there is a column of interpreted netsand. On the CPI-plot some of the netsands are marked with a blue circle. These are netsands that are unlikely contributors, and will not be counted as effective subzone height. Comparing netsands to the perforation intervals shown in the right margin it is seen that the (non-marked) netsands are fully perforated, and it is initially assumed that only netsand is perforated. The contributing (effective) height of a subzone is therefore calculated as the height in TVD of all the perforation intervals within the subzone, and then corrected for the reservoir dip:

$$h_i = \sum h_{pi} \cdot \cos(\alpha)$$

Where h_i is the height for subzone i, h_{pi} is the perforation height for perforation i within subzone i, and α is the dip angle of the reservoir.

However, in some sands there might be thin shales in between two sands, or sand/shale transitions that have too weak properties to produce. An example of this can be seen from P-8's CPI-plot (figure 12) for the first perforation interval in subzone 10.3. This means that using perforation intervals directly would overestimate the height. This effect can be accounted for by multiplying the above equation with a net to gross ratio (N/G) which is the height of producible sand divided by the total perforation height. The perforation intervals are of course fixed, and known heights. The producible height on the other hand depends on where we set the cutoff value for the permeability. Logging data are given per ½ foot, so intervals where the permeability is cut off will also be subtracted from the producing height. This is used to calculate the N/G. The correct equation for the subzone height therefore becomes:

$$h_i = \sum h_{pi} \cdot \cos(\alpha) \cdot N/G$$

Calculated subzone flowing heights for P-8 and P-12 are given in table 5 below:

Subzone	P-8 [m TST]	P-12 [m TST]
SN 10.3	4.4	-
SN 10.2	13.0	26.0
SN 10.1	12.6	7.9
SN 9.4	5.7	14.2
SN 9.3	5.4	10.6
Total	**41.1**	**58.7**

Table 5: Calculated subzone flowing height in m TST

3.6 Skin

The two wells both have fully perforated completions at the producing netsands where the perforation phasing (Θ_p) is low and shot density is high. Limited flow entry and perforation skin is therefore neglected, and skin is mainly evaluated from the given damage skin from the transient pressure test, and the negative pseudoskin effect from the well deviation. The skin damage is assumed constant over the producing intervals. However, it is known that damage skin is more dominating in less permeable formations, but there is no data available to account for this. There is also no change in well angle in the reservoir section.

For the producer the total skin has been calculated using the Cinco anisotropic model for deviation skin:

$$s_\theta = -\left(\frac{\tan^{-1}\left(\sqrt{\frac{k_v}{k_h}}\tan\theta\right)}{41}\right)^{2.06} - \left(\frac{\tan^{-1}\left(\sqrt{\frac{k_v}{k_h}}\tan\theta\right)}{56}\right)^{1.865} log\left[\frac{h_p}{100r_w}\left(\frac{k_h}{k_v}\right)^{1/3}\right] + s_\alpha$$

$$s_\alpha = \cos\left[\tan^{-1}\left(\sqrt{\frac{k_v}{k_h}}\tan\theta\right)\right] ln\frac{2\sqrt{\cos^2\theta + \frac{k_v}{k_h}\sin^2\theta}}{1+\sqrt{\cos^2\theta + \frac{k_v}{k_h}\sin^2\theta}}$$

and the total skin equation by Leif Larsen:

$$s_t = s_{LFE} + \frac{h}{h_p}s_d + s_\theta\left(\frac{L_p}{h}\right)^{2.7}$$

For the injector the calculation of total skin becomes more difficult because of temperature induced fractures from injecting cold(er) water into a hot formation. These fractures would create a negative pseudoskin, but is hard to calculate without knowing the number of fractures, the phasing between them and the length and diameter of the fractures – similar to the Karakas and Tariq mechanical/geometrical skin model [16]. Damage skin is low for the injector because of underbalanced perforation. A transient pressure buildup test shows that the negative pseudoskin component is larger (more negative) than that of the well deviation from the Cinco model alone. This is also supported by plotting injection rate versus bottomhole pressure, which makes it evident that the formation fractures. Fortunately the data from the transient test was good enough to interpret a total skin factor (log-log). Injection is below the OWC, so there is no need to account for mobility and relative permeability effects. Total skin factors are given in table 6 below:

Wells	**Total skin, s_t**
P-8	- 0.49
P-12	- 4.05

Table 6: Total skin values

It should be noted that even the total skin for the injector estimated from the buildup test might be overestimated (could be even more negative). This is because fractures might close at shutin when the buildup test is performed. It is often the case that initial injection logs shows better injectivity than theoretical values. Injectivity, however, usually gets worse with time because of plugging of the matrix.

3.7 Theoretical PI/II

Productivity/injectivity indices were calculated using the formula derived in the theory section and inserting the variables discussed in the previous sections:

$$PI = \frac{0.0536\, k_h h}{B\mu\left(ln\frac{r_e}{r_w} - \frac{3}{4} + s_t\right)}$$

Or similar for the calculations from mobility by modifying the above equation with $= \frac{k}{\mu}$:

$$PI = \frac{0.0536\, Mh}{B\left(ln\frac{r_e}{r_w} - \frac{3}{4} + s_t\right)}$$

3.7.1 Results

Depending on how the cutoff value for the permeability is determined, and where it is set, it will affect the average permeability, the producing height through the N/G, and hence the PI/II. A sensitivity analysis was performed by first calculating an initial average permeability and setting the cutoff value to a certain percentage of this for both geometric and arithmetic average. Another sensitivity analysis was performed by setting an absolute cutoff value. The sensitivity analysis is shown on the next page.

P-8 PI based on base case provided permeability and mobility:

P-8 PI based on base case provided permeability	
Subzone	**PI [Sm^3/d/bar]**
SN 10.3	1.4
SN 10.2	14.9
SN 10.1	10.4
SN 9.4	5.4
SN 9.3	3.4
Total	**35.5**

P-8 PI based on mobility	
Subzone	**PI [Sm^3/d/bar]**
SN 10.3	2.2
SN 10.2	13.5
SN 10.1	11.0
SN 9.4	1.8
SN 9.3	-
Total	**28.4**

Table 7: Results from PI calculations: Top calculation is based on permeability, and bottom calculation is based on mobility.

Absolute value of geometric average:

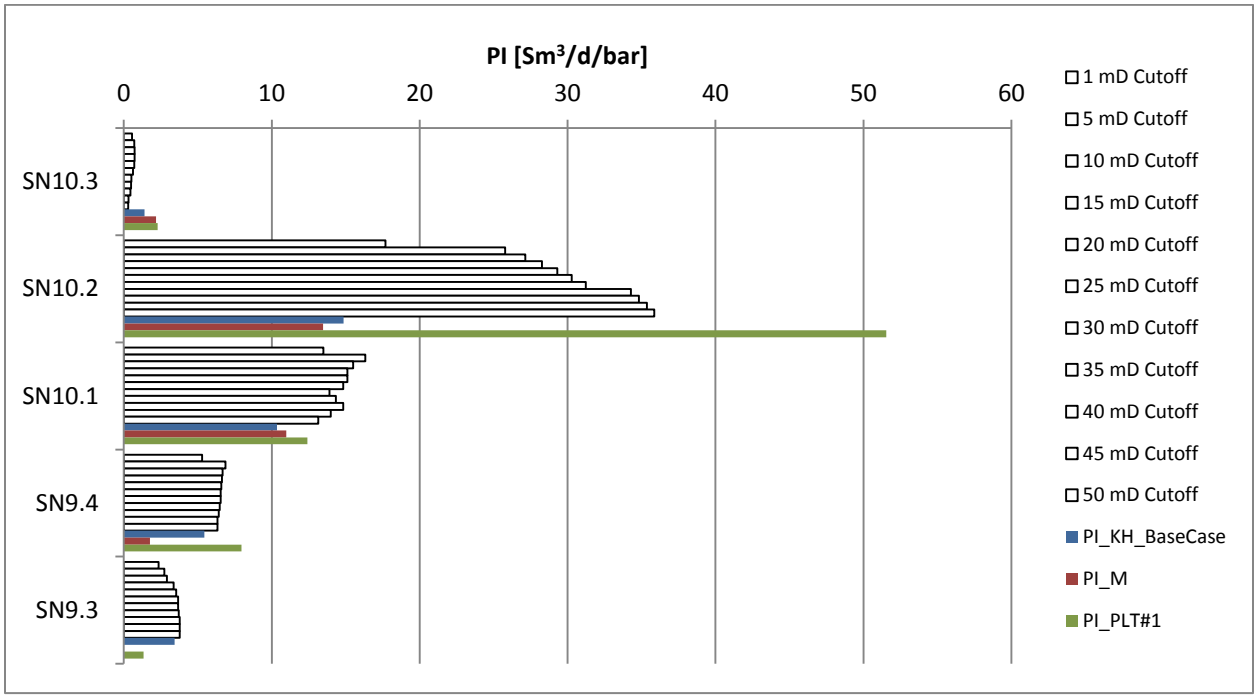

Figure 16: Sensitivity analysis for cutoff as absolute value of geometric average.

Percentage of arithmetic average:

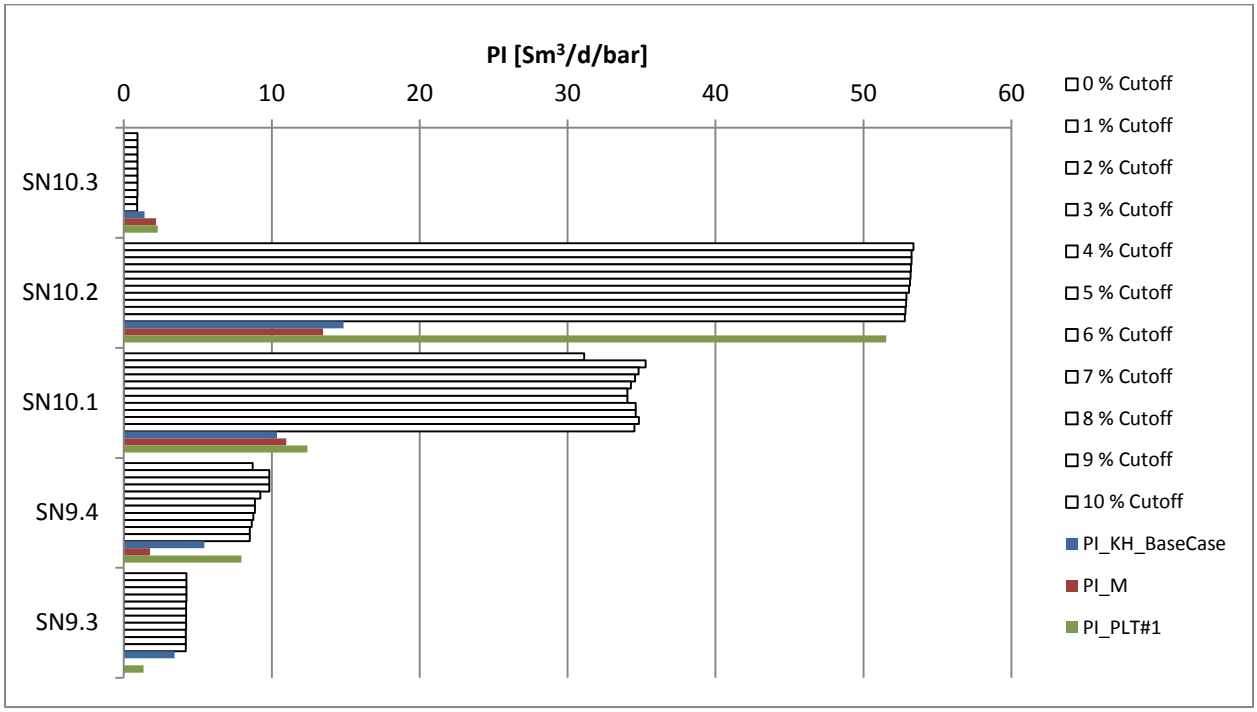

Figure 17: Sensitivity analysis for cutoff as percentage of initial arithmetic average.

Percentage of geometric average:

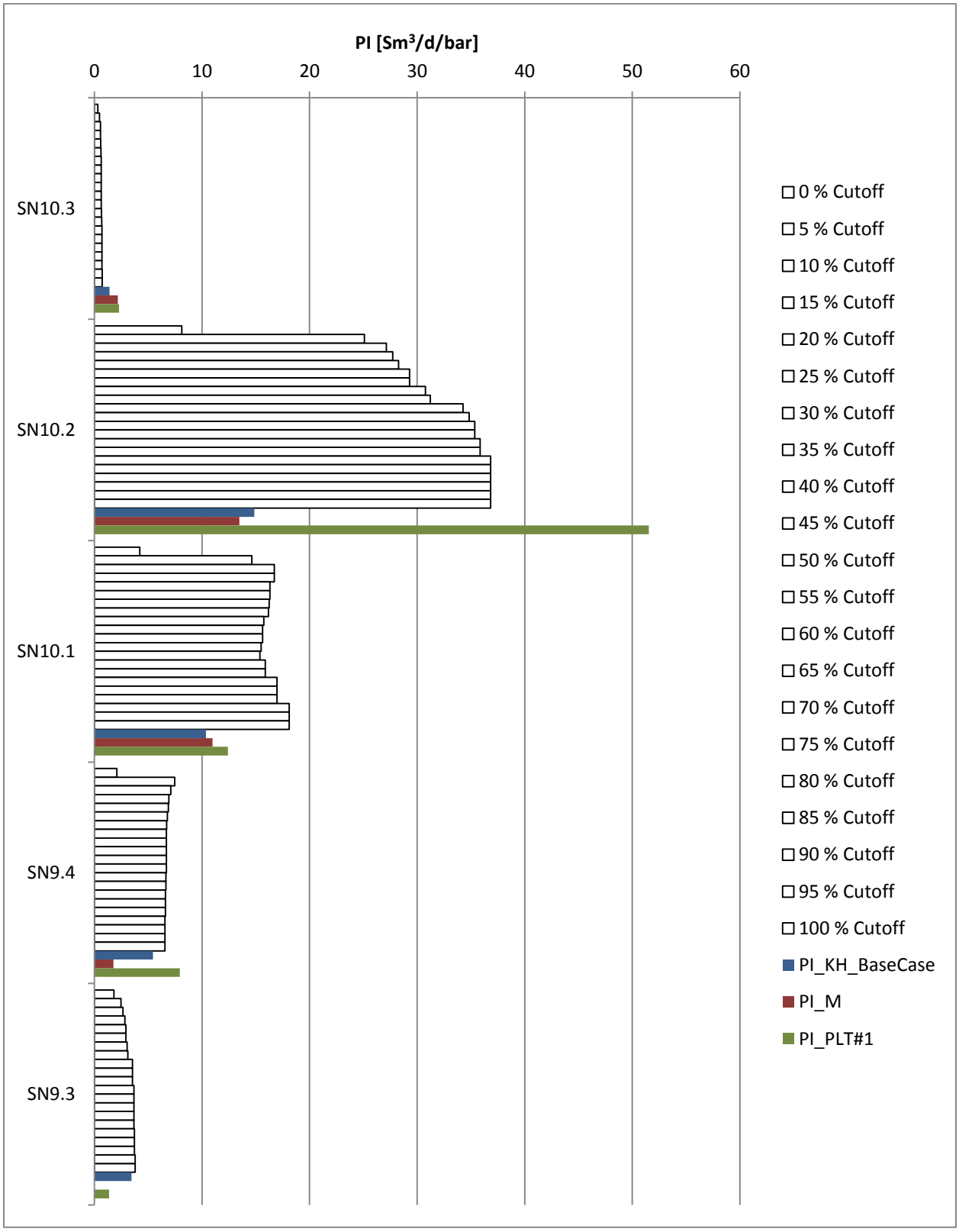

Figure 18: Sensitivity analysis for cutoff as percentage of initial geometric average.

Comparing the three models for determining the cutoff permeability and its effects on PI, it is clearly seen that while the arithmetic mean is almost spot on for some subzones, it can easily overestimate other subzones by a significant amount (e.g. SN 10.1). Both of the methods for geometric averages show roughly the same trends, but using an absolute cutoff will eventually eliminate low permeable subzones as the cutoff increases. This is seen in the top subzone SN 10.3 if the cutoff is increased even further. Because the permeability logs have limited resolution very good thin sands might disappear from the log. Such sands might contribute substantially to the zonal flow. Geometric averaged permeability using cutoff as a percentage of the initial geometric average where therefore chosen as the permeability model. This was also the model that estimated the theoretical total well PI closest to the PI from the PLT's.

Different cutoff strengths for the sensitivity analysis for the geometric average ranges from 0 to 100 %, in steps of 5%. Figure 18 show that increasing cutoff strength compared to actual PLT results has little effect for subzones SN 10.3, SN 9.4 and SN 9.3. Subzone SN 10.1 is most accurate at 65 % cutoff but there are no dramatic changes compared to surrounding steps. SN 10.2 has little change in PI after 50 % cutoff. Based on these observations, and the fact that uncertainty is apparent, it was decided to use a cutoff of 50 % of the initial geometric mean. PI calculations based on this cutoff are shown in the table below:

P-8 PI based on geometric permeability with 50 % cutoff	
Subzone	**PI [Sm^3/d/bar]**
SN 10.3	0.6
SN 10.2	34.8
SN 10.1	15.6
SN 9.4	6.7
SN 9.3	3.5
Total	**61.3**

Table 8: Results from PI-calculations based on the 50 % permeability cutoff model.

Similarly for the injector P-12:

P-12 II based on base case provided permeability	
Subzone	**II [Sm^3/d/bar]**
SN 10.2	7.8
SN 10.1	4.5
SN 9.4	2.9
SN 9.3	10.1
Total	**25.3**

P-12 II based on mobility	
Subzone	**II [Sm^3/d/bar]**
SN 10.2	26.2
SN 10.1	2.2
SN 9.4	7.9
SN 9.3	15.8
Total	**52.0**

Table 9: Results from II calculations: Top calculation is based on permeability, and bottom calculation is based on mobility.

P-12 II based on geometric permeability with 50 % cutoff	
Subzone	**II [Sm^3/d/bar]**
SN 10.2	19.0
SN 10.1	7.2
SN 9.4	6.6
SN 9.3	8.2
Total	**40.9**

Table 10: Results from II calculations based on the 50 % permeability cutoff model.

3.8 Timeline

The values calculated so far in the thesis are from initial well data available after drilling, wireline logging and initial well testing. They act as theoretical values and are important predictions of the performance that is expected from the wells and subzones. Before evaluating these data up against actual production data and logs it is important to have a picture of the main events that will affect production/injection efficiency. In this section important events are presented as a timeline:

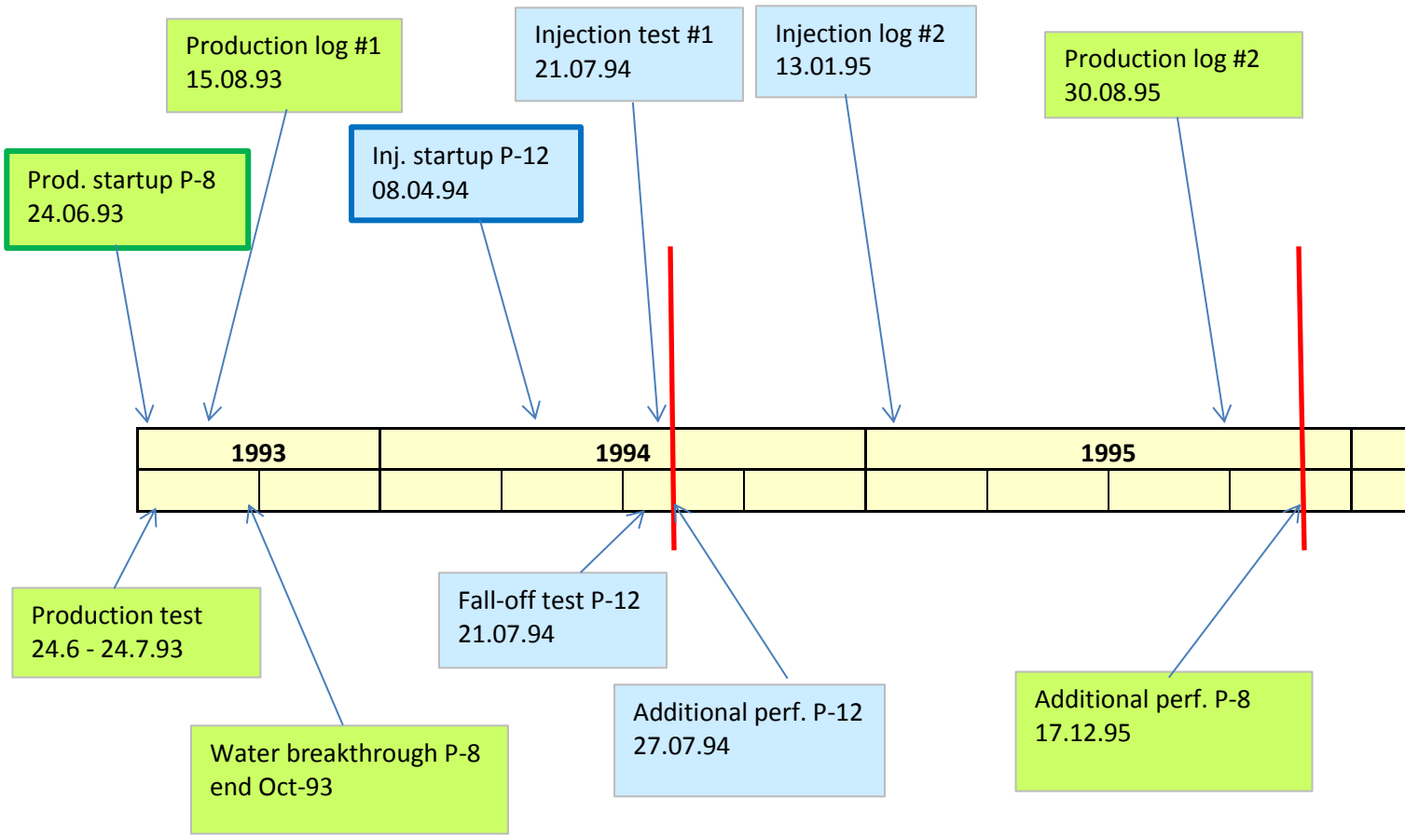

Figure 19: Timeline showing major events for the wells. Green boxes for producer, blue for injector.

Important events to notice in the timeline are:

- Startup of the producer
- First PLT before water breakthrough and before startup of the injector
- Startup of the injector
- PLT in the injector was performed after additional perforations were added
- Second PLT in the producer was performed after startup of the injector, but before additional perforations.

3.9 Production logs (PLT)

All of the PLT's are multirate logs, meaning they are measured at well shutin and at least one flowing rate. For this thesis concerning flow performance from the subzones we are only interested in the total liquid rate. For production optimization, at least as watercut increases, the phase splits would also become important in order to control zones that are contributing heavily with water and possibly limiting better zones. Production log results are given below:

P-8 PLT#1:

Subzones	Shut-in		High rate	
	P_{wf} [bar]	Q_o [Sm^3/d]	P_{wf} [bar]	Q_o [Sm^3/d]
SN 10.3	307.7	0	261.6	105
SN 10.2	310.0	-115	264.1	2250
SN 10.1	312.5	0	266.6	570
SN 9.4	315.3	0	268.9	370
SN 9.3	318.3	115	271.4	63

P-8 PLT#2:

Subzones	Shut-in		Low rate		High rate	
	P_{wf} [bar]	Q_{liq} [Sm^3/d]	P_{wf} [bar]	Q_{liq} [Sm^3/d]	P_{wf} [bar]	Q_{liq} [Sm^3/d]
SN 10.3	241.4	0	230.1	70	223.6	146
SN 10.2	241.4	-175	232.4	632	225.9	1357
SN 10.1	241.6	175	235.4	239	229.0	315
SN 9.4	246	0	238.6	153	231.3	223
SN 9.3	-	-	-	-	-	-

P-12 PLT#1:

Subzones	Shut-in		Low rate		Medium rate		High rate	
	P_{wf} [bar]	Q_w [Sm^3/d]	P_{wf} [bar]	Q_w [Sm^3/d]	P_{wf} [bar]	Q_w [Sm^3/d]	P_{wf} [bar]	Q_w [Sm^3/d]
SN 10.2	399.3	-190	429.3	880	471.5	1425	503.3	2510
SN 10.1	406.5	55	436.5	0	478.6	110	510.4	200
SN 9.4	409.0	135	438.9	0	480.8	490	512.9	950
SN 9.3	414.1	0	443.9	0	485.8	0	517.9	200

Table 11: PLT results

3.9.1 Flowprofiles

Flowprofiles are a popular way to visualize the PLT results and the contribution from each subzone. Flowprofiles have been made from Kappa Engineering's PLT interpretation software Emeraude, and are shown in figure 20 below:

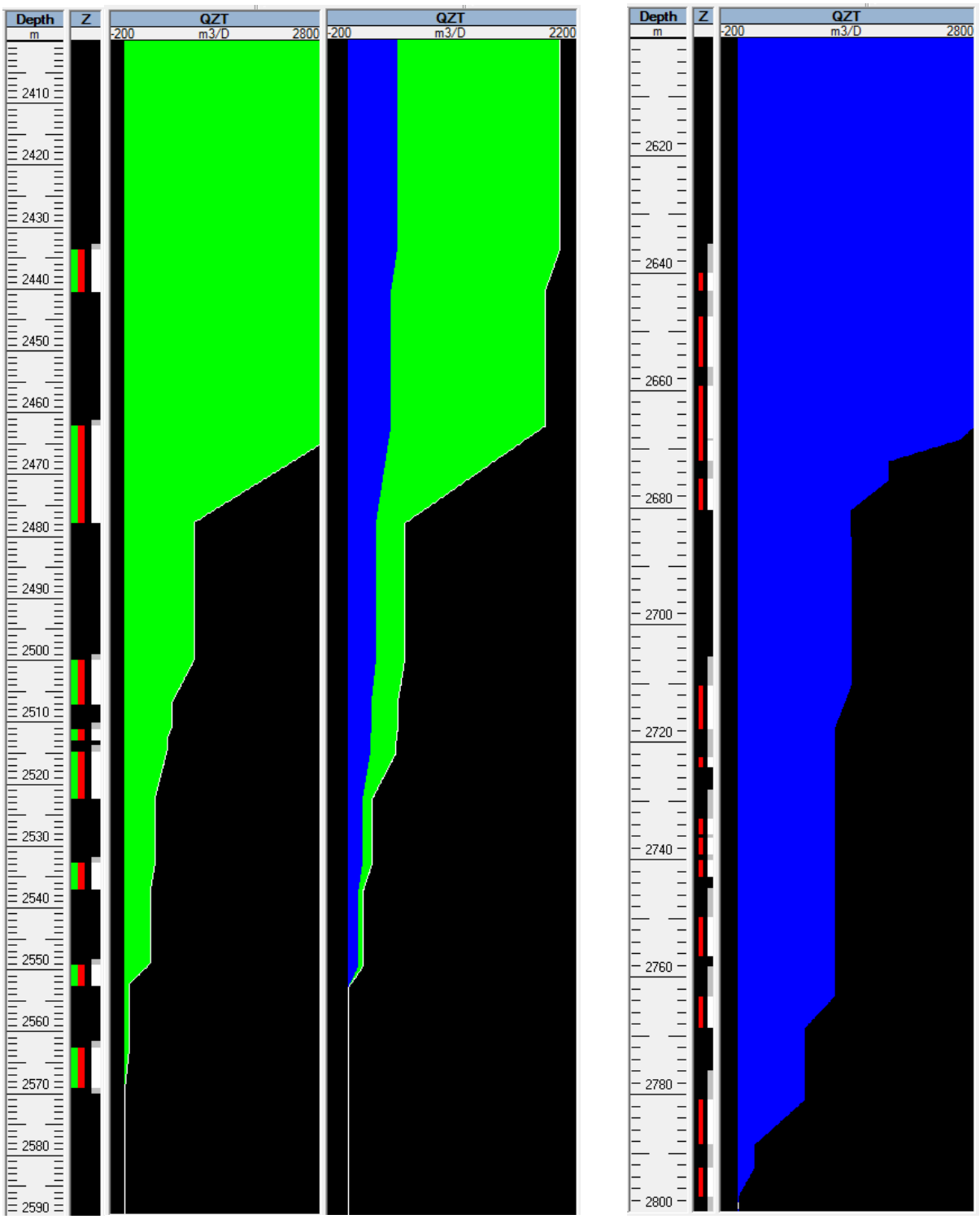

Figure 20: Flowprofiles. From the left: P-8 PLT#1, P-8 PLT#2, P-12 PLT#1

The PLT's and flowprofiles show that subzone SN 10.2 is by far the best producing zone, and is also taking the highest amount of water from the injector. A strange result is seen in PLT#1 in P-8 from the lowest subzone, SN 9.3. This zone is flowing during crossflow, but produces a weaker rate during the highrate test where the drawdown is higher. The result is unphysical, and a likely explanation is uncertainties in low flowrates, and that all of the 3 lowest subzones are contributing slightly.

3.9.2 SIP-analysis

SIP-analysis shows the reservoir pressure for each subzone, and shows the PLT results in terms of the productivity index (PI). As expected, subzone SN 10.2 has the highest PI.

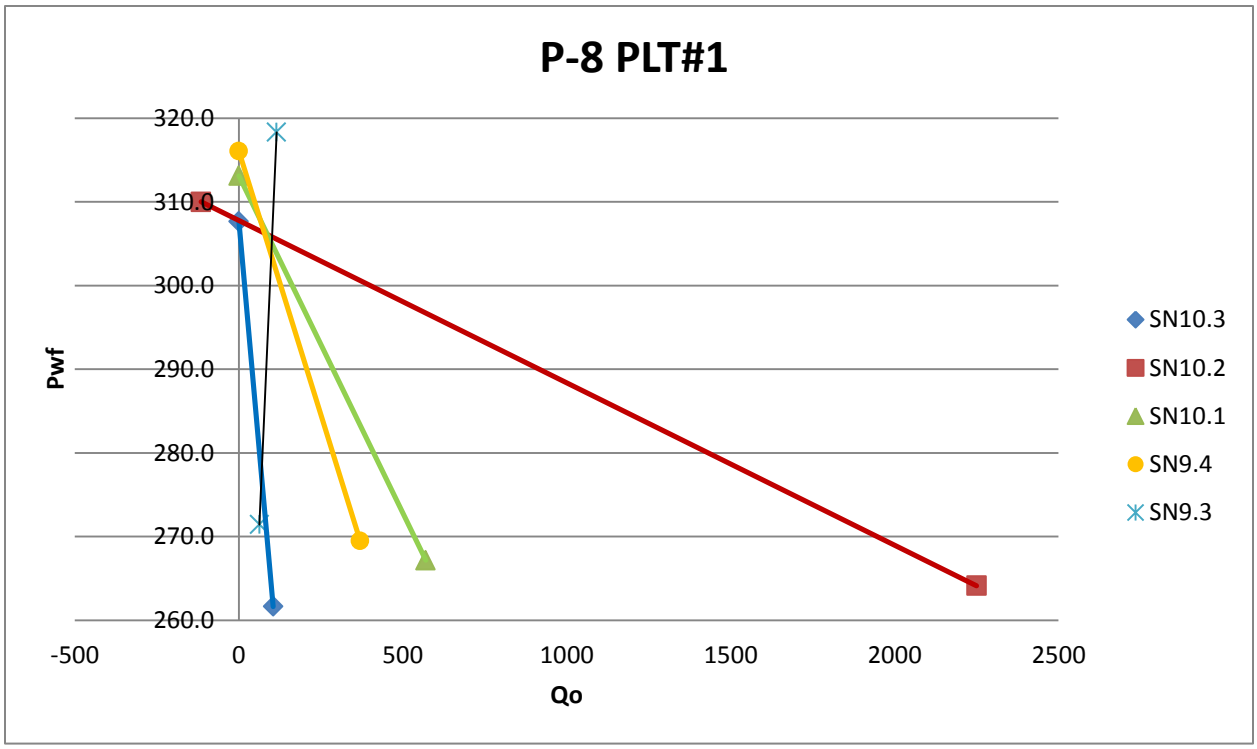

Figure 21: SIP-plot for P-8 initial PLT.

The unphysical PLT-result in SN 9.3 can also be observed in the SIP-plot where the gradient of the line is opposite of the expected. Reservoir pressure for this zone is assumed to be shut-in pressure.

Subzone	P_{res} [bar]	PI [$Sm^3/d/bar$]
SN 10.3	307.7	2.3
SN 10.2	307.8	51.5
SN 10.1	313.1	12.4
SN 9.4	316.1	7.9
SN 9.3	318.3	1.3
Total		**75.5**

Table 12: P-8 initial PLT reservoir pressure and PI.

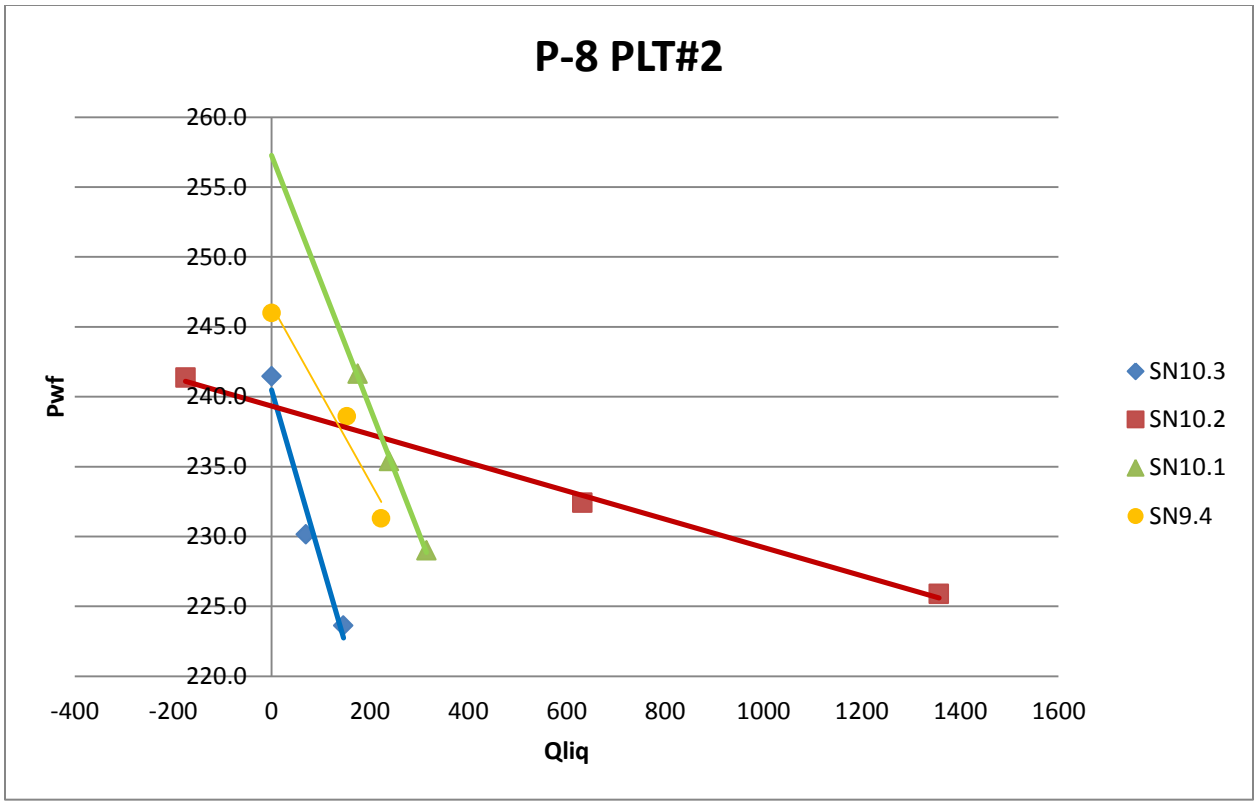

Figure 22: SIP-plot for P-9 PLT#2.

Subzone	P_{res} [bar]	PI [Sm^3/d/bar]
SN 10.3	240.5	8.2
SN 10.2	239.3	99.0
SN 10.1	257.3	11.1
SN 9.4	246.5	15.8
SN 9.3	-	0
Total		**134.2**

Table 13: P-8 PLT#2 reservoir pressure and PI.

PLT#2 in P-8 shows a depletion of the reservoir pressure and confirms the first PLTs performance of the zones relative to each other. However it also shows an improvement in absolute PI in all subzones, except SN 10.1 which is fairly stable. Especially The highest contributing subzone, SN 10.2, have almost doubled its PI after the startup of the injector.

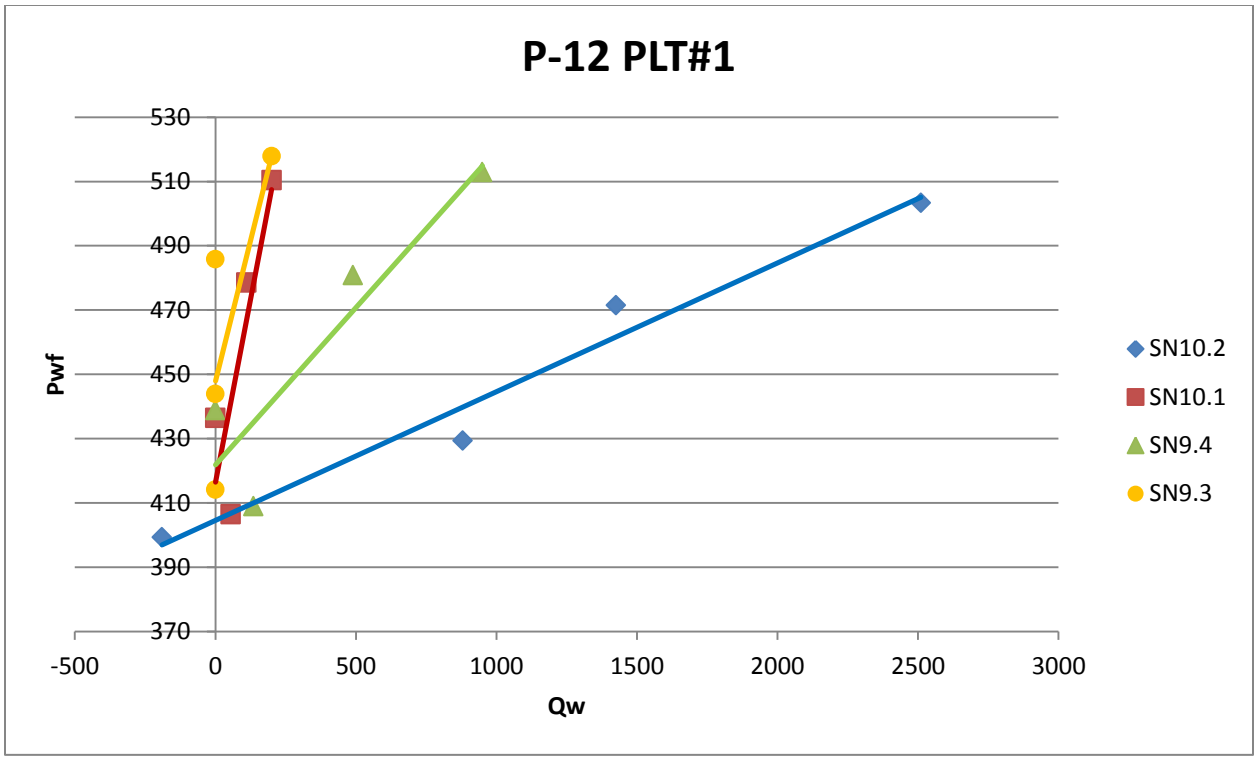

Figure 23: SIP-plot for P-12 PLT#1

The gradient of the lines in the SIP-plot for the injector is opposite of the producer. This is logical since a higher injection pressure would result in a higher injection rate.

Subzone	P_{res} [bar]	II [$Sm^3/d/bar$]
SN 10.2	404.5	24.9
SN 10.1	416.5	2.2
SN 9.4	421.8	10.2
SN 9.3	448.0	2.9
Total		**40.2**

Table 14: P-12 PLT reservoir pressure and II.

Injector, P-12, also shows the highest injectivity into subzone SN 10.2.

3.10 PI/II evaluation

In this segment theoretical PI calculations will be compared to the actual data from the production logs. The theoretical values should ideally act as the initial flow performance parameters. Therefore theoretical data are mainly compared to the initial PLT. However the first PLT are performed after about two months of production, and about 40 bars of reservoir pressure depletion. The second PLT in P-8 include the effects of the injector. Mobility data are not very accurate for the producer. This might be due to wettability and relative permeability effects between the measured fluid (often mud filtrate) and the oilzone.

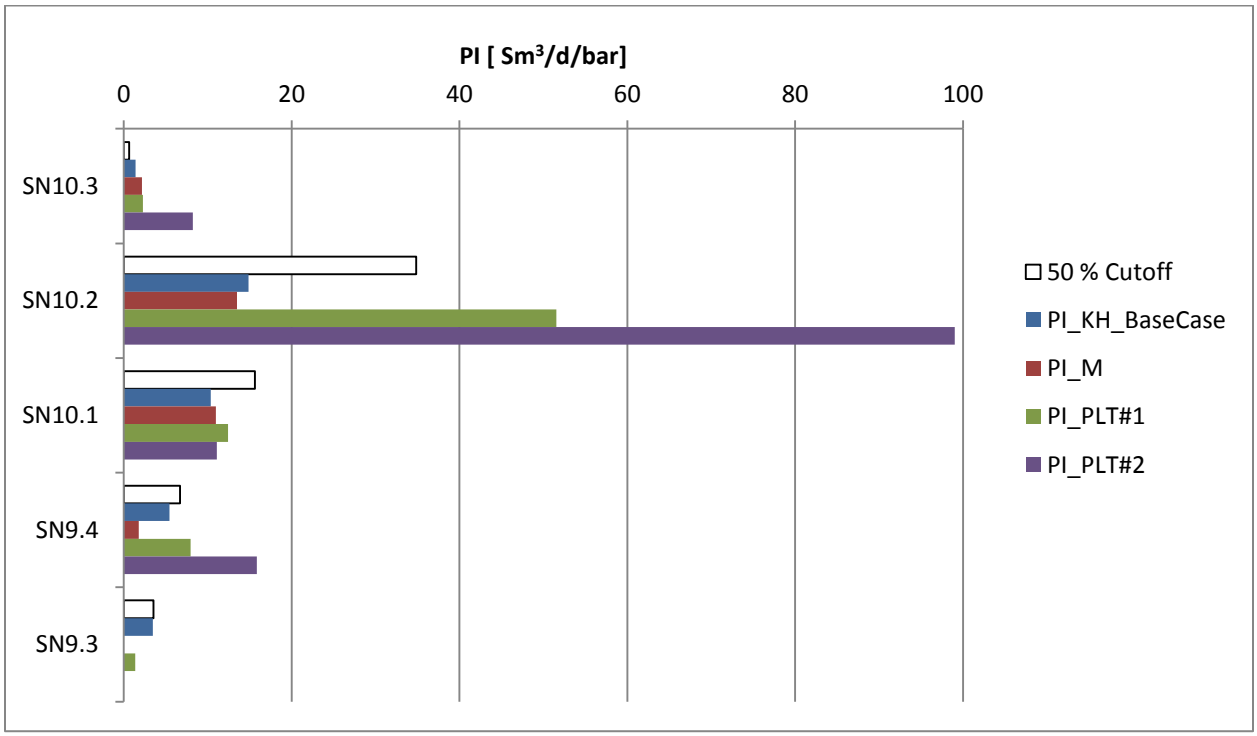

Figure 24: Theoretical PI estimates and PI from PLT results.

SN 10.3

Even though the injector, P-12, have not been perforated in subzone SN 10.3, it is clearly seen from the PLT results that there is some effect of the injector also in this subzone. A hypothesis for this subzone is that the well penetrates a thin good sand layer that is in communication with a bigger volume. This could explain why PLT#1 yields a better result than the theoretical calculations, and could also explain the unexpected contact to the injector.

SN 10.2

The new average permeability estimate based on a 50 % cutoff yields a significant improvement in theoretical PI for subzone SN 10.2. This is also the zone that shows the biggest improvement in PI, and is also by far the best volumetric rate contributor for the well.

SN 10.1

This is the only subzone where the theoretical PI estimated from mobility is on par. The theoretical calculations based on the cutoff permeability shows a slight overestimation of PI. Results from the two PLT's show that injector support is limited.

SN 9.4

Theoretical estimation based on the cutoff permeability model is on par with the first PLT. The second PLT shows effects from the injector.

SN 9.3

Theoretical PI seems overestimated for this subzone. The hypothesis is that the subzone volume is small. An explanation on why the first PLT shows a weaker result than theoretical calculations might be down to the elapsed production time and reservoir depletion. This is also supported by the second PLT where the zone has completely died, and clearly shows no communication with the injector.

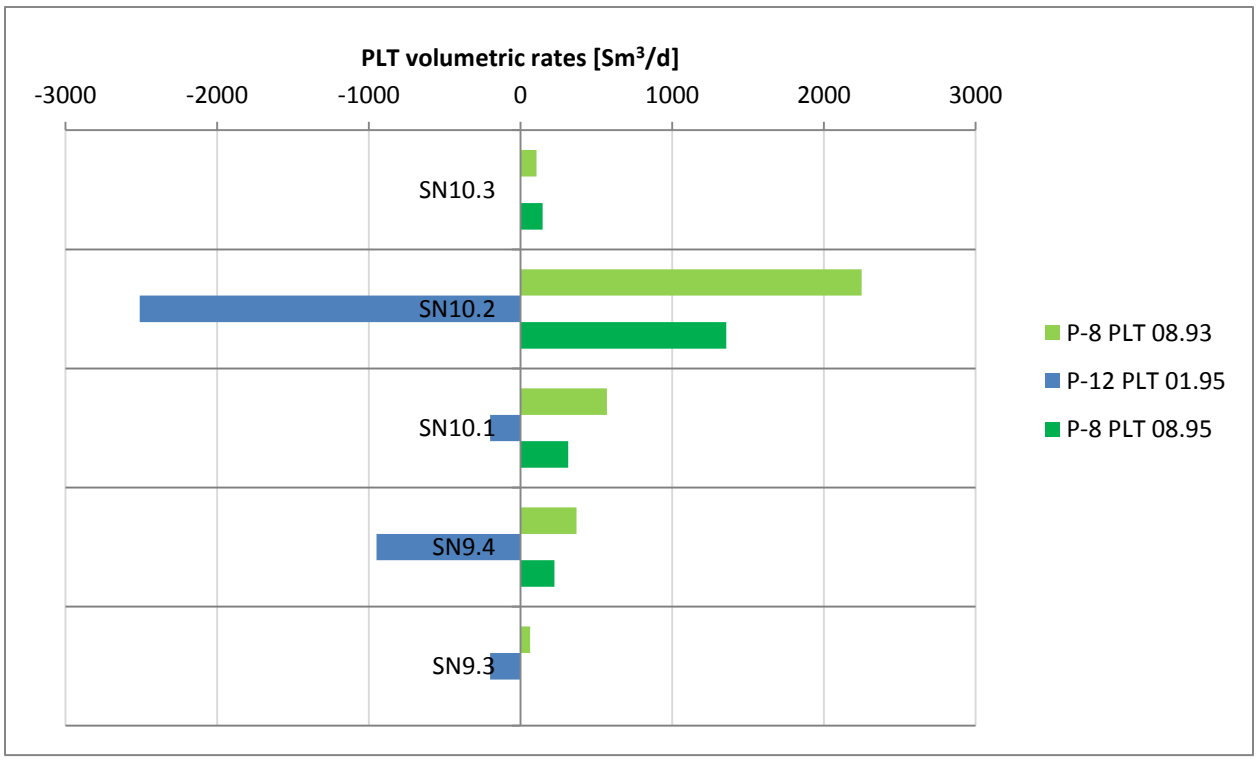

Figure 25: Volumetric PLT results for P-8 and P-12.

Figure 25 above supports many of the previous assumptions. It is easily seen that most of the water is being injected into SN 10.2, and that SN 10.1 gets very little water. The P-12 PLT confirms the results in SN 9.4. There is injection in SN 9.3 but there is probably no communication between the producer and the injector for this subzone, so no effects are seen in productivity. This supports that the producing volume in SN 9.3 probably is small.

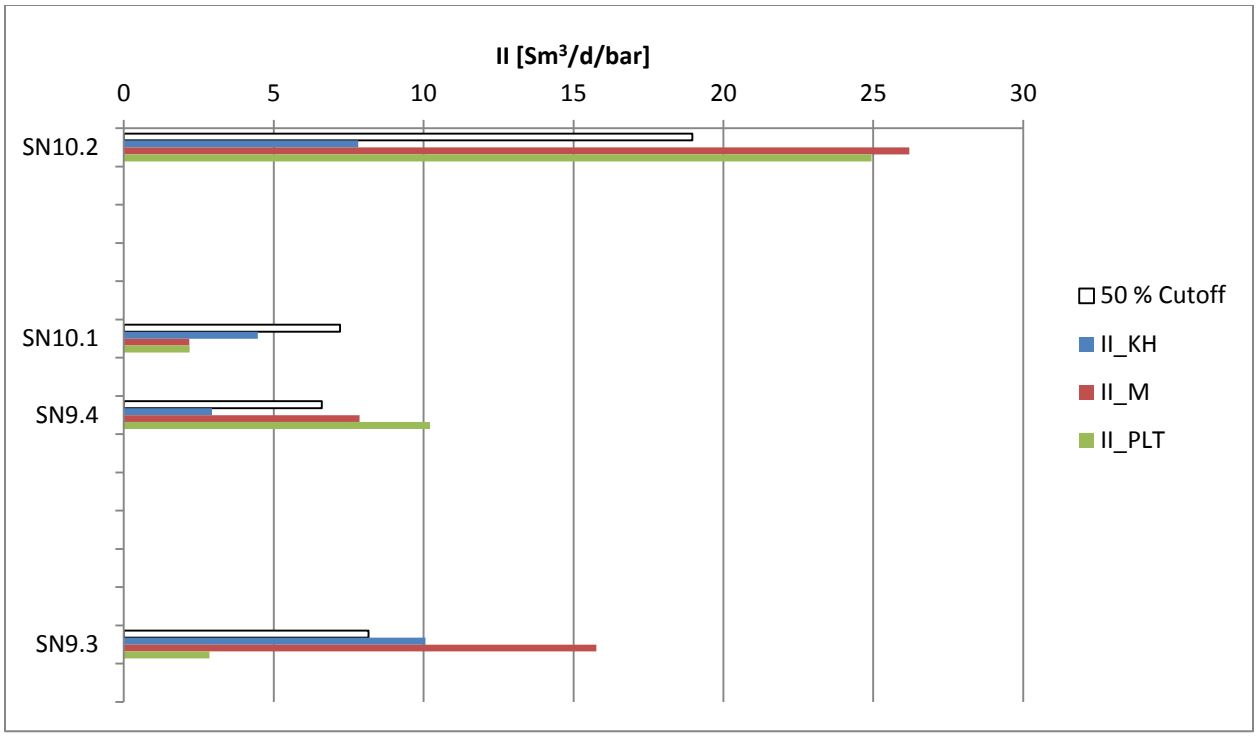

Figure 26: Theoretical II estimates and II from PLT results.

Figure 26 above show that the II calculated from mobility generally are very good for the injector, in contrast to the producer. The reason for this huge difference in reliability might be that relative permeability effects are small for the measured fluid (mud filtrate / water) in the water zone.

SN 10.2

This subzone show that the II calculated from the cutoff based permeability yields a huge improvement in theoretical accuracy compared to the provided permeability. As expected from the production data, this is also the best injection subzone.

SN 10.1

Mobility data is spot on for this subzone, while the calculations based on permeability overestimates the injectivity. A hypothesis for explaining this behavior might be formation damage. This would show on the mobility drawdown test, while it need not be apparent from the permeability log which is based on a porosity/permeability correlation. Limited (or restricted) reservoir volume, as suggested for this subzone from the producing side, might also be a reason for why the performance seen from the PLT is weaker than expected.

SN 9.4

Subzone SN 9.4 show the same result as subzone SN 10.2 where setting a cutoff value for permeability has a significant positive impact for the accuracy of theoretical estimate. Mobility data are even better.

SN 9.3

All theoretical calculations of injectivity overestimates this subzone. Especially the mobility is very far off compared to the other zones. Mobility data are local testpoints, and it is seen from the CPI that the

measurement were taken at a peak point. This would explain some of the difference in the II calculations from mobility compared to those from permeability. However even adjusting the mobility, would still overestimate the subzone. This is probably because the sand properties are good, but the volume is limited. This is also supported by the non-existing communication towards the producer. A small volume would build reservoir pressure more rapidly, hence reducing the injection “drawdown”.

It is not uncommon that actual injectivity performance is better than what is expected from initial theoretical data. The reason for this is thermal fracturing, as discussed briefly earlier. The two zones that have been overestimated with the cutoff permeability model are the same two zones that were overestimated on the producing side. The Producer also show decreasing PLT-results for these subzones. It is believed that flow restrictions/barriers are the reason for the behavior where SN 10.1 has limited communication between the two wells, and SN 9.4 shows no communication. The limited volumes would be more prone to pressure changes, and hence drawdown would be affected.

3.11 Conclusion

Initial flowprofiles are dominated by sandquality in the near wellbore area. In time flow performance will be dominated according to the reservoir volume that contacts the flowing sand. When injector support is established the flowprofiles will also be dominated by the degree of communication towards the injector.

Theoretical PI calculations based on mobility drawdown measurements should be used with care. The measurements are very local and limited in number, and even though the samples are carefully placed it is not certain that a sample will be representative for the sand. The samples are also known to be prone to near wellbore effects. However II calculations based on mobility can be good for the injector.

The theoretical PI calculations based on permeability are more stable. For the sake of flow performance it is shown through a sensitivity analysis that selecting a permeability cutoff of 50 % of the initial subzone geometric average permeability can improve the estimation accuracy. Cutting away low permeable sand also needs to be accounted for in the subzone flowing height through a revised N/G. The main argument for this approach is that experience shows that inflow performance is dominated by the good sands in a subzone.

It is also important to include a total skin factor rather than just the damage skin. For wells that have fully perforated netsands with dense perforations (and low phasing) LFE and perforation skin can be neglected without significant error. Many wells in Snorre are deviated wells, and for these wells it is important to include the negative skin from the deviation. It is important to keep in mind the reservoir dip, and when calculating deviation skin the well angle should be given with respect to the stratigraphic surface.

Calculations imply that subzones with flow restrictions easily can be overestimated. Subzones with smaller volumes are more prone to pressure changes and will show a more rapid pressure depletion for the producer, and a quicker buildup of reservoir pressure for the injector. This will affect the drawdown, and hence the PI. There is no way to get data on flow restrictions without performing transient tests. For most wells on Snorre such tests are not available, and cannot be accounted for at the initial phase. PLT's are therefore important to get accurate information about flow performance, and a correct image of the flowprofiles of the wells.

Nomenclature:

Sm^3 – m^3 at standard conditions
MSm^3 – Million Sm^3
o.e. – Oil equivalents
Gp. – Group
Fm. – Formation
N/G – Net to Gross ratio
TVD – True Vertical Depth (from mean sea level unless otherwise stated)
WAG – Water Alternating Gas (injection)
ICV – Inflow Control Valve (aka. DIACS)
MDT – Modular formation Dynamics Tester (Schlumberger wireline logging tool)
GOR – Gas to Oil Ratio
WC – Water Cut
PI – productivity Index
II – Injectivity Index
TST – True Stratigraphic Thickness
LFE – Limited Flow Entry
IPR – Inflow Performance Relation
SIP – Selective Inflow performance (analysis)
PLT – Production Logging Tool
RPS – Revolutions Per Second
STOOIP – Stocktank Oil Originally In Place
OWC – Oil/Water Contact
CPI – Computer Processed Interpretation (of well logs)
P-8 – Platform well in slot # 8 (producer)
P-12 – Platform well in slot # 12 (injector)

p – pressure
p_{wf} – well flowing pressure
t – time
V – volume
ϕ – porosity
h – flowing sand height
h_s – vertical spacing of perforations
h_p – height of perforation interval (TST)
h_1 – height between top sand and top perforation interval (TST)
q – volumetric rate
B_o – oil formation volume factor
B_w – water formation volume factor
c_t – total system compressibility
k_x – permeability in x direction
k_y – permeability in y direction
k_z – permeability in z direction
k_r – permeability in radial direction
k_h – permeability in horizontal direction
k_v – permeability in vertical direction
k_d – permeability in damaged zone
k_{cz} – permeability in crushed zone
k_{rw} – relative permeability for water
k_{ro} – relative permeability for oil
ρ_o – oil density
ρ_w – water density
μ_o – oil viscosity
μ_w – water viscosity
r – radius
r_w – wellbore radius
r_e – outer drainage radius
r_d – damaged zone thickness
r_{cz} – crushed zone thickness
s_t – total skin factor
s_d – damage skin
s_p – perforation (completion) skin
s_h – horizontal skin component
s_v – vertical skin component
s_{wb} – wellbore skin
s_{sz} – crushed zone skin
s_{LFE} – limited flow entry skin
s_θ – deviation skin
l_p – perforation (shot) length
L_p – length of perforation interval (MD)
z_p – height between bottom sand and mid perforation interval (TST)
θ – well angle with respect to res. dip
θ_p – perforation shot phasing
α – dip angle of reservoir
α_θ – Karakas and Tariq table value
a_1 - Karakas and Tariq table value
a_2 - Karakas and Tariq table value
b_1 - Karakas and Tariq table value
b_2 - Karakas and Tariq table value
c_1 - Karakas and Tariq table value
c_2 - Karakas and Tariq table value
K_0 – modified Bessel function of second type and zero order
M_{ow} – mobility ratio oil/water
S_{or} – residual oil saturation
S_w – water saturation

Subscript D: dimensionless

Table of figures:

Table of tables

References:

[1] Internal Statoil web: «Snorre på vei mot 2040»
http://entry.statoil.no/NewsAndMedia/News/2010/Pages/25AugSnorre2040_2.aspx

[2] Internal Statoil web: «20 år i ryggen – nær 30 år igjen»
http://entry.statoil.no/Organisation/Units/64946/News/Pages/080312Snorre20År.aspx

Official Statoil webpage about Snorre:
http://www.statoil.com/no/OurOperations/ExplorationProd/ncs/snorre/Pages/default.aspx

[3] NPD facts about Snorre
http://factpages.npd.no/ReportServer?/FactPages/PageView/field&rs:Command=Render&rc:Toolbar=false&rc:Parameters=f&NpdId=43718&IpAddress=143.97.2.35&CultureCode=en

[4] "Long Range Reservoir Management Plan Snorre Unit"
Internal link: http://sp-st04.statoil.com/sites/f3be3275-708d-47f7-bdfc-5f03480549e5/LRMP%20Snorre%202012/Document%20library/Forms/DispForm.aspx?ID=17&RootFolder=%2Fsites%2Ff3be3275%2D708d%2D47f7%2Dbdfc%2D5f03480549e5%2FLRMP%20Snorre%202012%2FDocument%20library

[5]"SPE Meeting 140911 – Snorre Field Development presentation"
Internal link: http://sp-st03.statoil.com/sites/4715f412-059c-4dac-864b-8e0940a29e7d/Document%20library/Forms/DispForm.aspx?ID=342&RootFolder=%2Fsites%2F4715f412%2D059c%2D4dac%2D864b%2D8e0940a29e7d%2FDocument%20library

[6] Leif Larsen (1998) – "Brønntesting – Analyser av Trykktransiente Data". Compendium for Statoil and UiS (HiS at the time, course MPE350).

[7] Odeh, A.S. (1980) – "An Equation for Calculation Skin Factor Due to Restricted Entry" JPT ID: 8879-PA

[8] Streltsova-Adams (1979) – "Pressure Drawdown in a Well With Limited Flow Entry" SPE ID: 7486-PA

[9] Gui, Zhang, Cunha (2008) – "A Theoretical and Numerical Investigation of the Pseudoskin Factor" PetSoC ID: 08-05-48

[10] Lee, Kyonggi (2001) – "A New Method for computing Pseudoskin Factor for a Partially-Penetrating Well" SPE ID: 68698

[11] Roemershauser, Hawkins (1955) –"The Effect of Slant Hole, Drainhole, and Lateral Hole Drilling on Well Productivity" SPE ID: 437-G

[12] Conco, Miller, Ramey (1975) – "Unsteady-State Pressure Distribution Created By a Directionally Drilled Well" SPE ID: 5131-MS

[13] Wong, Harrington, Cinco-Ley (1986) – "Application of the Pressure-Derivative Function in the Pressure-Transient Testing of Fractured Wells" SPE ID: 13056-PA

[14] Clifford, Pucknell (1991) – “Calculation of Total Skin Factors” SPE ID: 23100

[15] Haddad et al. (Schlumberger) (2000) – “So What is the Reservoir Permeability?” SPE ID: 63138

[16] Karakas, Tariq (1991) – “Semianalytical Productivity Models for Perforated Completions” SPE ID: 18247

Appendix

Karakas and Tariq [16] table values for perforation skin calculations:

Horizontal dependency on phasing	
Perforation phasing, θ_p	α_θ
0 (360)	0.250
180	0.500
120	0.648
90	0.726
60	0.813
45	0.860

Vertical skin correlation coefficients				
Perforation phasing, θ_p	a_1	a_2	b_1	b_2
0 (360)	-2.091	0.0453	5.1313	1.8672
180	-2.025	0.0943	3.0373	1.8115
120	-2.018	0.0634	1.6136	1.7770
90	-1.905	0.1038	1.5674	1.6935
60	-1.898	0.1023	1.3654	1.6490
45	-1.788	0.2398	1.1915	1.6392

Wellbore skin correlation coefficients		
Perforation phasing, θ_p	c_1	c_2
0 (360)	1.6×10^{-1}	2.675
180	2.6×10^{-2}	4.532
120	6.6×10^{-3}	5.320
90	1.9×10^{-3}	6.155
60	3.0×10^{-4}	7.509
45	4.6×10^{-5}	8.791

Table A1: Karakas and Tariq table values for perforation pseudoskin.